Chem Soc Rev

RSC Publishing

REVIEW ARTICLE

View Article Online
View Journal | View Issue

Cite this: *Chem. Soc. Rev.*, 2013, **42**, 6959

Forward and pressure retarded osmosis: potential solutions for global challenges in energy and water supply†

Chalida Klaysom,[a] Tazhi Y. Cath,[b] Tom Depuydt[a] and Ivo F. J. Vankelecom*[a]

Received 6th February 2013

DOI: 10.1039/c3cs60051c

www.rsc.org/csr

Osmotically driven membrane processes (ODMP) have gained renewed interest in recent years and they might become a potential solution for the world's most challenging problems of water and energy scarcity. Though the concept of utilizing osmotic pressure difference between high and low salinity streams across semipermeable membranes has been explored for several decades, lack of optimal membranes and draw solutions hindered competition between forward osmosis (FO) and pressure retarded osmosis (PRO) with existing water purification and power generation technologies, respectively. Driven by growing global water scarcity and by energy cost and negative environmental impacts, novel membranes and draw solutions are being developed for ODMPs, mass and heat transfer in osmotic process are becoming better understood, and new applications of ODMPs are emerging. Therefore, OMDPs might become promising green technologies to provide clean water and clean energy from abundantly available renewable resources. This review focuses primarily on new insights into osmotic membrane transport mechanisms and on novel membranes and draw solutions that are currently being developed. Furthermore, the effects of operating conditions on the overall performance of osmotic membranes will be highlighted and future perspectives will be presented.

[a] *Centre for Surface Chemistry and Catalysis, Faculty of Bioengineering Sciences, Katholieke Universiteit Leuven, Kasteelpark Arenberg 23, Post Box 2461, 3001 Leuven, Belgium. E-mail: ivo.vankelecom@biw.kuleuven.be; Fax: +32 16 321998; Tel: +32 16 321594*

[b] *Division of Environmental Science and Engineering, Colorado School of Mines, 1500 Illinois Street, Golden, Colorado 80401, USA*

† Electronic supplementary information (ESI) available. See DOI: 10.1039/c3cs60051c

Chalida Klaysom

Chalida Klaysom received her PhD in Chemical Engineering from Australian Institute of Bio-engineering and Nanotechnology, the University of Queensland, on the fabrication of novel composite ion-exchange membranes. After her graduation, she joined the Center for Surface Chemistry and Catalysis, KU Leuven, where she is currently a postdoctoral scholar to continue her research in membrane technologies. Her current research interests include membrane development using the concept of composite materials for diverse applications, such as water purification, desalination, energy/power production, and gas separation.

Tazhi Y. Cath

Dr Cath is an associate professor of environmental engineering at the Colorado School of Mines. His main fields of research are membrane processes for wastewater treatment, desalination of saline and hypersaline brines, reclamation of impaired water for potable reuse, and energy from water and wastewater. Dr Cath is a PI on many research projects focusing on the integration of membrane contactor processes in seawater and brackish water desalination, in domestic and industrial wastewater treatment, and in life support systems. He is currently the director of the Advanced Water Technology Center (AQWATEC) at Colorado School of Mines.

1. Introduction

Growing population, increasing water demand and impairment, and rising energy use over the past decades stimulated exploration of alternative water and energy resources. Emerging osmotically driven membrane processes (ODMPs) might provide sustainable solutions for the global needs of both clean water and clean energy.[1–7] ODMPs utilize the osmotic pressure difference of solutions across a semipermeable synthetic membrane to draw water from a dilute feed solution to a more concentrated draw solution. The two ODMPs that draw most attention in recent years are forward osmosis (FO) and pressure retarded osmosis (PRO).[8–10] While FO and PRO use similar physical principles and process components, they are very different from the application perspective. FO uses the osmotic pressure difference across the membrane to extract clean water and to concentrate (reduce the volume) impaired feed streams, or to dilute the concentrated draw solution stream for downstream processing, with minimal energy consumption (*e.g.*, osmotic dilution).[11] PRO, on the other hand, facilitates conversion of osmotic pressure difference to hydraulic pressure, thus enabling generation of useful work (*e.g.*, electricity) when releasing the hydraulic pressure through a turbine or other devices. As such, PRO is a unique membrane process – its main objective is to generate power, rather than to perform chemical separation.

Unlike pressure-driven membrane processes such as reverse osmosis (RO), nanofiltration (NF), and even ultrafiltration (UF) or microfiltration (MF), FO requires minimal external energy input, mainly for liquid circulation. Yet, an energy input is needed if a synthetic draw solution requires a reconcentration process for water recovery and draw solution reuse in the process.[12–14] Other advantages of FO over pressure-driven membrane processes include low fouling tendency and minimal pre-treatment of the feed, reduced cake layer formation which simplifies membrane cleaning, and low-pressure operation which simplifies design and equipment used.

PRO is a unique membrane process. This is because unlike other membrane processes that perform separation, it can facilitate the capturing and conversion of the energy of mixing into a useful energy source.[15] For example, a tremendous potential energy source exists in each estuary, where river water meets the ocean, or in every seawater desalination plant that discharges concentrated brines into the ocean. This energy could potentially be harvested for power generation using PRO. It was estimated that these potential sources of energy can generate approximately 2000 TWh per year of electric power, which is more than 10% of the current world energy demand.[8] Moreover, PRO is considered a clean technology because negligible chemical use or CO_2 emissions are involved in the process of energy generation.

FO and PRO use the same type of semipermeable membrane, which is different in structure from thin film composite membranes used for RO and NF. Due to the low performance of first generation ODMP membranes, which are a key element for both FO and PRO, the processes were for a long time considered inferior to existing membrane technologies. Recent research and development of membranes and draw solutions for ODMPs, and the better understanding of mass transport of solutes and solvents during osmosis have further increased the interests and consideration of osmotic processes as viable technologies that can utilize renewable resources as a driving force to produce clean water and clean and renewable energy from currently untapped resources.

This review starts with a broad background on osmosis and engineered osmosis, covering the main ODMPs (*i.e.*, FO and PRO) and closely related processes such as osmotic dilution, RO, and hybrid processes comprising the above and other processes. Subsequently, progress in the development of new membranes and draw solutions is presented and discussed. Special topics are covered, including a review of theoretical studies of membrane transport phenomena and transport modelling, and an overview of membrane and draw solution developments. Several new approaches for development of osmotic membranes and draw solutions are highlighted. PRO has been recently briefly reviewed, based on its timeline historical development,[8] and some recent reviews on FO have been published.[9,16–18] As they have focused mainly on potential applications, this review mentions this aspect only briefly. The link between PRO and FO is emphasized and materials and modelling aspects are discussed in detail.

Ivo F. J. Vankelecom

Ivo Vankelecom (Ninove, Belgium, 1967) studied Bioscience Engineering at the Catholic University of Leuven (KU Leuven), Belgium, where he graduated in 1990. In 1994, he obtained his PhD in Applied Biological Sciences from the Department of Interphase Chemistry on "Inorganic Porous Fillers in Organic Polymer Membranes". He subsequently worked at KU Leuven as a postdoc on membrane catalysis. During this period, he spent 6 months at the Ben-Gurion University of the Negev (Beersheva, Israel) in 1999 and at Imperial College (London, England) in 2001. Since 2002, he has been a professor at KU Leuven where he teaches membrane technology, adsorption and chromatography. He is the author of more than 150 peer-reviewed papers and 16 patents.

2. Classification of osmotic processes

Osmosis is the transport of solvent (mostly water) through a semipermeable barrier/membrane from a feed stream of high solvent concentration/activity (*i.e.*, low solute concentration) to a stream of lower solvent concentration/activity (*i.e.*, high solute concentration). The receiving solution is termed draw solution. Different terms, such as osmotic agent, osmotic media, or brine were used for draw solution in the early literature, but the term

Table 1 Comparison between RO, FO, and PRO

	RO	FO	PRO
Driving force	• External hydraulic pressure (P)	• Osmotic pressure	• Osmotic pressure
Main application	• Water purification process • Desalination	• Water purification process • Desalination	• Power production
Operating condition	• $P \sim$ 10–70 bar • Brackish and seawater feed solution • pH 6–7	• $P \sim$ atmospheric • Brackish, seawater or some synthetic draw solutions, such as aqueous NH_3 • Impaired water, seawater or other feed solution • pH 6–11	• $P \sim$ 10–15 bar • River, brackish, seawater, and brine solution • pH 6–7
Desirable membrane property			
(1) Physical morphology	• Dense top layer and porous sub-layer • Good thermal and mechanical stability	• Thin membranes with dense active layer on porous, low torturous sub-layer	• Thin membranes with dense active layer on porous, low torturous sub-layer
(2) Chemical property	• Good chemical stability to chloride solution	• Very hydrophilic • Good chemical stability to chloride solution and synthetic draw solution	• Very hydrophilic
(3) Membrane requirement	• High water permeability • High solute retention • Robust for high pressure operation	• High water permeability • High solute retention • Stable in synthetic draw solution	• High water permeability • Good solute retention to maintain osmotic pressure driving force • Strong enough for the external applied pressure
Target performance	• High flux (at around 4–5 μm s^{-1})	• High flux and good water recovery	• High power density (>5 W m^{-2})
Challenges	• Energy consumption • Operating cost	• Internal concentration polarization • Suitable draw solution • Draw solution recovery and re-concentration	• Internal concentration polarization • Module design • Membrane cleaning • Feed stream pre-treatment

draw solution is currently exclusively used. Osmotic pressure is defined as the hydrostatic pressure required for stopping the diffusion of the solvent through the membrane. When using osmosis in engineered systems, two basic osmotically driven membrane processes are commonly practiced: FO and PRO. Recent studies focused on the osmotic dilution (ODN) process.[11,19] While this is also an engineered ODMP, it is practically osmosis.

Though RO, FO, and PRO share common characteristics as membrane technologies, solute and water flow directions are different, as well as the driving forces for mass transport. RO is classified as a pressure driven membrane process because the driving force is an external hydraulic pressure. In FO and PRO, on the other hand, water flux is driven by the net osmotic pressure difference across the membranes. Therefore, there are different requirements for membranes to be suitable for each process.

Comparison between RO, FO, and PRO systems is provided in Table 1. When considering the operating conditions of each system, seawater RO (SWRO) membranes require high mechanical strength to withstand the high applied pressures, while FO and PRO operate at much lower pressures and thus require lower mechanical strengths. Typical RO membranes consist of a thin selective layer on top of a porous structure that allows the fast passage of water, which may be further supported by an even more open backing fabric. Water flux and solute retention by RO-type membranes are determined mainly by the top skin layer, and the porous support layers only provide the mechanical strength to the membranes to facilitate operation at high pressures. The flux through FO and PRO membranes on the other hand is driven by the osmotic pressure difference ($\Delta\pi$) across the membrane, in which the properties of the support layer play a crucial role in flux and performance of the system. While water is mechanically ''pushed'' though the support layer in RO, water chemically diffuses through the membrane in FO and PRO; thus, the presence of unwetted pores or gas trapped inside the pores of the support layer in FO or PRO membranes, and internal concentration polarization (ICP), can induce dramatic flux decline in FO and PRO. ICP is a transport phenomenon inside the porous support layer of the membrane during FO and PRO in which dilution of the draw solution in the pores substantially reduces the osmotic pressure driving force across the membrane.[20,21]

Though FO and PRO are closely related processes, they still require a different degree of selectivity for the membrane skin layer. FO requires highly selective membranes, while PRO aims to obtain high power density and thus requires just enough salt rejection to govern concentration polarization and maintain the driving force.[22] In addition, membranes for PRO have to be strong enough to withstand the hydraulic pressure of the draw solution.

In a way, PRO can be viewed as the transition process from FO to RO in the osmotic processes.[9,23]

3. Historical developments

Though the engineered osmosis concept has been proposed more than half a century ago,[15] its development has been relatively slow. It took almost 20 years since the launch of the concept in 1954 to gain interest from researchers. This was due to the insufficient progress in membrane science at that time. It was due to the oil crisis in the early 1970s that more attention was drawn from researchers to explore more energy resources and to search for new, low-energy processes for water purification.[8] The historical developments in osmotic membrane processes are summarized in Fig. 1.

Early studies focused on theoretical feasibility of the PRO process.[15,23–31] However, limited experimental PRO studies were performed due to the complexity of the system compared to RO and FO.[21,32] Therefore, the main approach was to develop models to predict PRO performance from RO and FO experiments using commercially available RO or NF membranes.[20,23,31,33–37] These early studies in the 1980's addressed the critical impact of ICP on the osmotic membrane processes.[21,23,28] Some FO applications for agricultural purposes, food processing, and wastewater treatments were explored.[38–41] The concept of using volatile solutes as draw solutions to extract water from seawater was introduced in 1965, and investigation of such draw solutes and their recovery processes started in the 1970s.[39,42–46] Once Hydration Technology Innovation (HTI) (formerly Osmotek and Hydration Technology Inc.) (Albany, Oregon) introduced, the first commercial cellulose triacetate (CTA) FO membrane, more new emerging applications were proposed and the search for suitable draw solutions became more intensive. Subsequently, the understanding of the fundamentals of ODMPs was profoundly developed. Nevertheless, the development of membranes specially designed for osmotic membrane processes just took off very

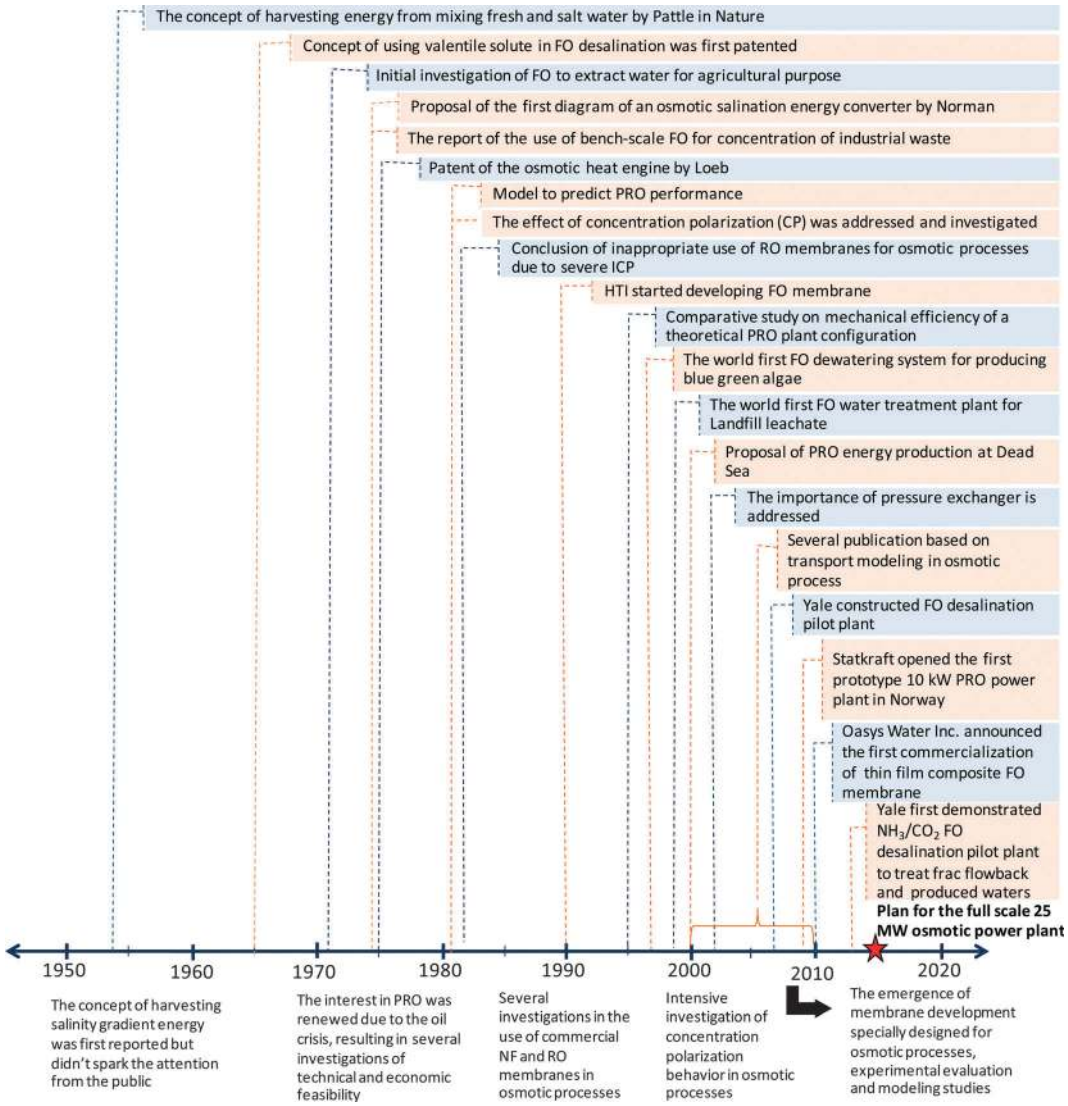

Fig. 1 Historical development in osmotic membrane processes.

recently and gained more attention after the big step forward taken by Yale university in 2007 (*i.e.*, construction of an ammonia–carbon dioxide draw solution pilot-scale system for FO seawater desalination) and by Statkraft (Norway) in 2009 (*i.e.*, construction of the first PRO power plant). The current focus in membrane development for ODMPs is on thin film composite (TFC) membranes due to their superior performance over the asymmetric cellulose acetate membranes. In 2010, Oasys Water Inc., announced the first commercial TFC membranes.[47,48] Recently, this membrane was challenged in an NH_3–CO_2 FO desalination pilot study that treated high salinity water produced from natural gas extraction operation in the Marcellus shale (USA).[49] The energy used in the pilot plant was estimated to be less than 50% of that estimated for a conventional evaporative desalination. This demonstration opened up a new potential application of ODMPs, which further stimulates ODMP developments.

4. ODMP applications

ODMPs can be used in many applications, including water production, food and pharmaceutical processing, industrial and domestic wastewater treatment, and energy production.[2,8,11,12,16,32,38,39,46,50–72] In this section an overview of potential applications of the osmotic processes (especially FO) is discussed. More comprehensive reviews on the potential applications of ODMPs are provided in previous publications.[9,16–18]

Major advantages of FO over RO are the potentially lower energy consumption and higher fouling resistance of the FO process. Working at very low hydraulic pressure, fouling layers are much less compacted in FO and can be easily removed by osmotic backwashing[73–75] or very mild periodic chemical cleaning; thus, many of the possible FO applications can be operated with low quality feed water, including domestic and industrial raw wastewater.[76–78] However, the main challenge in FO is the recovery of the draw solution, which is the major energy consumption step in FO. Besides the widely studied FO desalination process, where separation of water from the draw solution solutes is required, applications of FO can be further divided into two, based on their purposes – whether it is used to dilute the draw solution or to concentrate the feed solution (Fig. 2).

A novel idea of directly using diluted draw solution from FO has widened the applications of FO and at the same time eliminated the main disadvantage of draw solution reconcentration.

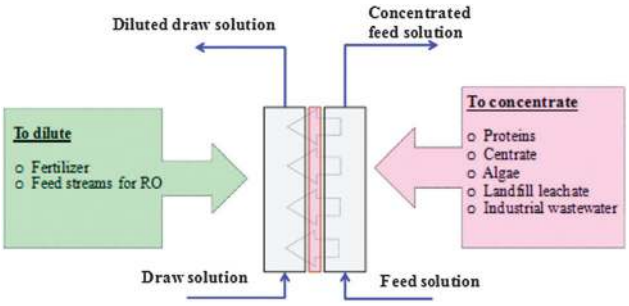

Fig. 2 Diversity of FO applications.

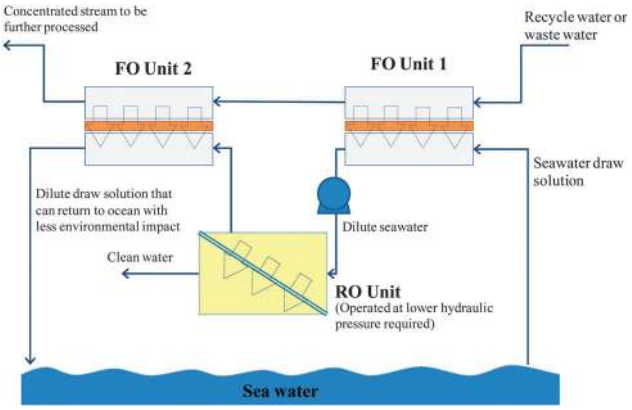

Fig. 3 Schematic drawing of a hybrid FO–RO process for 'water augmentation' (adapted from Cath *et al.*[11,80–82] and Bamaga *et al.*[51])

This concept of osmotic dilution offers several advantages, including (1) versatile water resources can be used as long as their osmotic pressures are lower than that of the draw solution; thus, the process can be applied in an area even where fresh water resources are limited, and (2) no separation of the draw solution is required, making the process energy-friendly.

FO was recently studied for dilution of concentrated solutions of fertilizers which were then directly applied for fertigation.[79] FO was also tested for concentration of dilute streams of proteins in pharmaceutical applications and microalgae in algal biodiesel production, for concentration of industrial waste and centrate from anaerobic digesters, or for recovery of water from landfill leachates before being further treated and/or disposed to the environment.[52,59,79] Furthermore, the concept of hybrid FO–RO, combining wastewater treatment and desalination was currently proposed.[11,52,80–83] The general design of the hybrid FO–RO is illustrated in Fig. 3.

FO–RO hybrids show high potential for water treatment in various industries, especially along coastal locations, because the feed solutions for the FO can be very diverse and the product can be highly purified. The process consists of one open loop for wastewater treatment (as the feed stream for two FO units) and a closed loop for seawater in desalination (draw solution for the FO unit). Seawater is used as the draw solution for the first FO unit and is thus diluted before entering the RO desalination plant, hence lowering the energy required for the RO desalination. The RO concentrate is then fed to a second FO unit as the draw solution. The brine from RO is diluted by the second FO unit before being discharged, thus reducing environmental impacts. Simultaneously, the wastewater feed from the first FO is further concentrated and thus its volume minimized for further treatment.

Most FO applications are still explored at a laboratory scale. Further detailed investigations and conceptual proofs are required in order to turn FO into a mainstream treatment process.

5. Draw solutions

Draw solution is the working fluid in ODMPs and is responsible for providing the driving force for the processes. The two main

Table 2 Promising draw solutions and their recovery methods

Draw solutes	Recovery	Advantage	Disadvantage
Inorganic			
NaCl, $MgCl_2$, $NaSO_4$[14]	NF, RO, distillation	Inexpensive solute; readily available	Difficult separation
Removable solute by pH adjustment (*i.e.*, metal carbonates, oxalates or tartrates)[45]	pH change to induce precipitation and filtration	Cheap production cost	High capital investment
$Al_2(SO_4)_3$[44]	Multi-state chemical precipitation	Comparable product purity compared to RO	High chemical demand Large-scale process design
Thermolytic/volatile			
SO_2[42]	Heated gas stripping	Inexpensive recovery process	Toxic
NH_3–CO_2[62,87,100]	Heating (60 °C) results in thermolysis	High solubility in water and high ODF Reconcentration with low-grade heat	Toxic thermolytic product, NH_3; diffusive loss
Organic			
Alcohols[43,86]	Distillation		Difficult separation
Glucose (and other sugars)[39,46]	None necessary	No separation necessary	Limited application
Albumin[101]	Denaturation and solidification upon heating	High solubility in water	Low ODF
2-Methylimidazole-based compounds[97]	FO-MD	Designable to increase ODF	Increasing ICP with further modification
Magnesium acetate (and other organic salts)[95]	Biodegraded in FOMBR	Carbon source	Limited application
Polymer-based			
Polyethylene glycol (PEG)[96]	UF or NF	Easy recovery	Low ODF
Cloud point solute such as PEG-derived fatty acids[99]	Cloud point precipitation and filtration	High ODF	Require heating unit/temperature control
Polyacrylic acid[98]	UF	High ODF through dissociation of surface groups	Increased viscosity
Charged dendrimer[101]	UF	High ODF through dissociation of surface groups	Multiple-step synthesis
Hydrogel[88,89]	De-swelling by heating or pressurization	Sunlight irradiation for de-swelling	Low water flux
Magnetic nanoparticles[90–93,102]	Magnetic field or UF	No reverse solute flux and easy recovery	Aggregation during recycle

Notes: ODF = Osmotic Driving Force.

challenges associated with draw solutions include finding a suitable solution that provides a strong driving force for mass transport and the energy consumption associated with reconcentrating the draw solution for continuous FO operation.[14] Thus, besides developing membranes suitable for ODMPs, the search for suitable draw solutions is of great importance. The key criteria for the selection of a draw solution include: (1) the draw solution should have high osmotic pressure, (2) the reverse diffusion of the draw solutes (leakage through the membrane into the feed) should be minimal, (3) the draw solutions can be easily and economically reconcentrated and water recovered, (4) the draw solution must not be toxic, and (5) it should be inexpensive.[14,84] Moreover, the draw solution should not degrade the membranes and should not cause scaling or fouling on the membrane surface. A number of solutions, either naturally available or synthetic, were proposed for use as draw solutions in past studies.[14,39,42–45,61,62,84–99] Some promising draw solutions and their recovery methods are summarized in Table 2.

The draw solutes can be classified into four major categories: inorganic solutes, thermolytic/volatile solutes, organic solutes, and polymer-based macro-solutes.

5.1 Inorganic solutes

Inorganic salts are most widely used draw solutes in FO and PRO research due to three major advantages, which include being abundantly available in nature, inexpensive, and having high osmotic pressure that can induce high water flux in FO and PRO.

Most inorganic salts can generate high osmotic pressure and could be potentially used as draw solutions. Achilli *et al.* recently developed a protocol for selecting suitable inorganic salts to use as the draw solutions for FO.[14] More than 500 inorganic compounds

were screened by three initial criteria: chemical solubility and chemical hazard, available osmotic pressure, and cost per liter of the draw agents needed for producing an osmotic pressure of 2.8 MPa. Only 14 candidates survived the first screening. These candidates were further tested in FO with commercial HTI membranes. Among those solutes, $KHCO_3$, $MgSO_4$ and $NaHCO_3$ proved to be most promising to provide a good performance (high flux and low ICP) and a low replenishment cost. However, these draw solutes contain ions such as Mg^{2+}, SO_4^{2-}, and CO_3^{2-} that have high risk of scaling; thus, their applications are restricted. NaCl, abundantly available at low cost, remains popular in the literature.

Inorganic salt recovery normally requires a distillation or membrane process such as RO or NF and therefore the energy footprint accounts for one of the major drawbacks of using inorganic salts as draw solutes.[14,85] A few specific cases allow less energy intensive separation methods to be used.[62,87]

Solidification could also be a viable separation mechanism. In the case of $CaCO_3$ and $Al_2(SO_4)_3$, precipitation can be induced through a change of pH or the addition of a flocculant (*e.g.*, $Ca(OH)_2$), respectively.[44,45] Recently, Liu *et al.* obtained purified water using $Al_2(SO_4)_3$ as the draw solute and CaO as the flocculant.[61] The resulting gel-like structure was easily separated from the water by adding negatively charged silica-coated magnetic nanoparticles and applying a magnetic field. Addition of sulphuric acid restored the reagents to their original state. Finally, Phuntsho *et al.* investigated the draw solute properties of a number of salts commonly used as fertilizers.[103] The resulting diluted draw solution could be readily applied as a clean fertilizer solution, making recovery unnecessary.

5.2 Thermolytic/volatile solutes

Thermolytic salts are a special type of draw solutions, consisting of highly soluble gases or volatile solutes that can generate high osmotic pressure and can be easily recovered. The draw solutes can be evaporated and regenerated by using low temperature from low grade or waste heat sources (*e.g.*, power plants). SO_2 was the first volatile solute to be tested for FO desalination and its recovery method was patented in 1965.[42] SO_2 can be easily recovered by gas stripping, but could not be implemented in desalination processes due to its toxicity.[42] Another thermolytic solution, like the NH_3–CO_2 mixture, is one of the most studied thermolytic draw solutions. High draw solution concentrations can be generated by adjusting the ratio of gases that form the ammonium salt.[87,100] It was estimated that with 6 M draw solution (on CO_2 basis), an osmotic pressure of more than 30 MPa (300 bar) can be generated, which is far greater than that of seawater.[49,100] Furthermore, the draw solution can be easily recovered by boiling out the NH_3 and CO_2 at approximately 58 °C. It was claimed that this process consumed less than 10% of the energy required in RO desalination.[2] This allows the use of the NH_3–CO_2 FO system to treat water with high salinity contents that most other membrane technologies fail to achieve economically. Despite all the advantages of the NH_3–CO_2 draw solution, there is a critical concern over the quality of the water produced by the process. To meet the standard drinking water quality, NH_3 is required to be removed to concentrations below 2 mg L^{-1}. This would require the development of new membranes chemically stable in such draw solution environments. Though it is considered to be a promising draw solute, this solution is also restricted for use in the drinking water production due to safety aspects. Other membrane filtration units, such as RO, might be required to be combined with the NH_3–CO_2 FO process in order to bring the salt content down to the standard water quality requirements.[49]

5.3 Organic solutes

Although not as common as inorganic solutes, several organic compounds have been tested as draw solutes as well. These include ethanol, butanone, humic acid, and sugars such as glucose or fructose.[39,43,46,86,96] As these organic solutes are not electrolytes, water fluxes are much lower in FO, especially for larger draw solution compounds such as albumin.[101] However, their main advantage is that they can be experimentally designed to obtain specific, desirable physiochemical properties such as solubility, diffusivity, and size suitable for different ODMPs. For example, Yen *et al.* employed different 2-methylimidazole-based compounds as a draw solute and found that an oligomer electrolyte derivative generated a higher water flux and lower reverse solute flux than the original 2-methylimidazole.[97] This was possible through the addition of the electrolyte group, increasing the total solute concentration after dissociation in solution. The increase in molecular size, result of the oligomerization, hindered permeation through the membrane active layer and thus decreased reverse solute flux.[97] Specifically in osmotic membrane bioreactors (OMBRs), the use of organic solutes can be more advantageous than that of inorganic salts. The latter will start accumulating in the feed compartment after reverse salt flux, thereby affecting membrane operation and sludge wasting frequency. If organic solutes (*e.g.*, magnesium acetate) are used, the leaked draw solution solute will be biodegraded by microorganisms, thereby preventing accumulation.[95]

Recovery of organic draw solutions can be problematic, requiring distillation or even denaturation and loss of the draw solute in the case of albumin.[43,86,101] However, organic solutes can serve as great draw solutions in certain applications that do not necessitate separation; for example, sugars serve a secondary goal when the diluted draw solution also serves as a nutritious drink.[39,46] Another concern associated with the use of organic solutes for draw solution is their susceptibility to biological degradation. Ironically, this can also prove advantageous, for example, in the use of magnesium acetate as draw solution in OMBR processes. After use as a draw solution, they serve as a carbon source for microorganisms.[95]

5.4 Polymer-based solutes

It is clear that the separation of the solute from the diluted draw solution is a major hurdle when either organic or inorganic solutes are used for draw solutions. Therefore, recent studies also focus on polymer-based macrosolutes, which allow easier recovery, for example with UF.[98] In addition, their molecular structure and size can be manipulated to achieve solutions with high osmotic pressure and desired performance.[95,98,104]

Even when an unmodified polymer was used, like polyethylene glycol, a reasonable water flux of 1.75 μm s^{-1} (6.3 L m^{-2} h^{-1}) could be attained. Recovery of up to 97% of the draw solute with UF was possible, although high concentrations of the draw solute were detrimental to water flux, because of the osmotic effect.[96] Recently, an FO process using PEG-derived fatty acids draw solutes was patented.[99] In this approach, recovery is possible through temperature-induced cloud point initiation or lowering of the cloud point through the addition of an insoluble gas. To further increase the osmotic pressure, linear polymers and dendrimers can also be modified to polyelectrolytes. As an example, the use of a poly(sodium acrylate) (PSA) draw solute showed multiple advantages. Water flux comparable to that of a seawater draw solution was reached and reverse salt flux was substantially lower. After regeneration of the draw solution with UF, less than 0.4% of water flux in FO was lost after each run of the recycle.[98]

Recently, another promising hydrogel based draw solution was synthesized. Hydrogels are cross-linked three-dimensional polymers containing hydrophilic groups that possess high internal osmotic pressure that can entrap large amounts of water.[88] The dewatering of the swollen hydrogels can be easily achieved using stimuli such as pH, pressure, temperature, and light to change the form of the hydrogels, thereby releasing water. Li *et al.* investigated the use of carbon black-hydrogel composites as a draw solution in FO.[89] Sunlight irradiation was used as the stimulus for dewatering. Water was completely recovered within 40 min of exposure to sunlight; however, the FO water flux of this system was still relatively low (0.21 μm s^{-1}/ 0.76 L m^{-2} h^{-1}).

With present advances in nanotechnology, superparamagnetic nanoparticles were proposed to be used as the draw solution for FO.[13,91,93] The separation of the superparamagnetic nanoparticles can be easily achieved using a magnetic field within less than 3 min, depending on particle size and field strength. Reasonable water fluxes of up to 2.9 μm s^{-1} (10.4 L m^{-2} h^{-1}) were obtained with polyacrylic acid-covered particles. However, after regeneration of the draw solute, water flux quickly declined due to particle aggregation. The stability of the superparamagnetic nanoparticles clearly still needs further improvement.

This overview illustrates how diverse the research of draw solutions has been. While this diversity is proof of the possibilities of future research into draw solutions, certain issues have to be taken into consideration as well. First, there is no perfect draw solution. Different treatment objectives and solute recovery technologies dictate different draw solutions, as illustrated in many cases.[7,13,17,27] Second, the lack of a standard evaluation method for draw solute performance greatly hinders comparison. This could be facilitated if a set of criteria, much like the one used by Achilli *et al.*,[14] were to be implemented to derive a solute's properties in FO. And finally, future attention should be directed towards not only new, easily separable draw solutes, but also possible new recovery technologies, of which membrane distillation is an example.[18,32]

6. Mass transport phenomena in ODMPs

While ODMPs are relatively simple processes, mass transport through ODMP membranes is complex and depends on many parameters including membrane type, structure, and orientation, temperatures and compositions of the feed and draw solutions, hydraulics, and more. Prior to describing the mass transport mechanisms in ODMPs, it is worth reviewing the terms used throughout this review. The terms ''FO'' and ''PRO'' are used to refer to the two basic ODMPs. While FO is operated with negligible hydraulic pressure (transmembrane pressure), PRO works at a transmembrane hydraulic pressure (higher draw solution hydraulic pressure) lower than the transmembrane osmotic pressure to allow diffusion of water from the feed into the draw solution (Fig. 4a and b). In ODMPs, there are two different orientations in which the membrane is

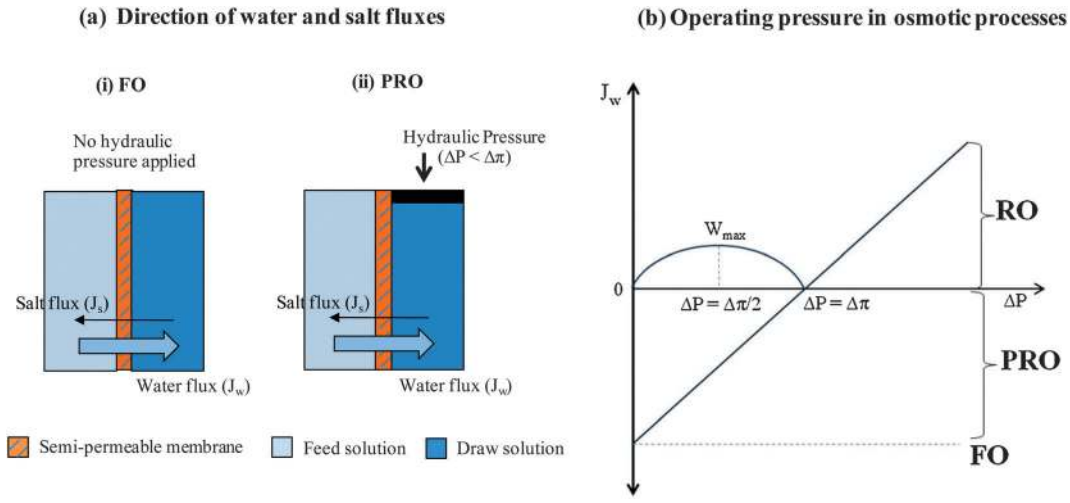

Fig. 4 (a) Direction of water and salt fluxes for (i) FO and (ii) PRO processes, and (b) the magnitude of water flux and PRO power output as a function of operating pressure.

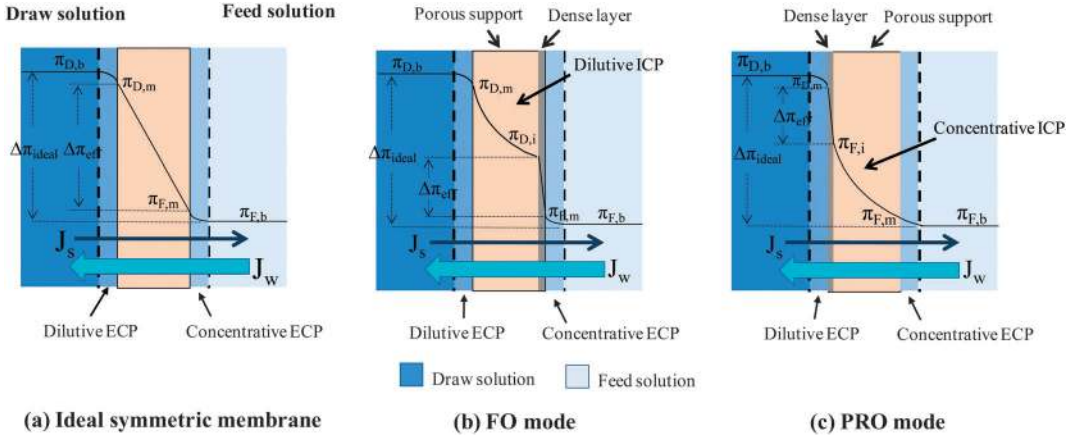

Fig. 5 Schematic diagrams of external and internal concentration polarization developed (a) in a symmetric membrane, (b) in an asymmetric membrane in FO operating mode, and (c) in an asymmetric membrane in PRO operating mode (adapted from Lee *et al.*[23] and Phillip *et al.*[106]).

utilized in the processes. The common orientation in which the active layer of the membrane is in contact with the feed solution (Fig. 5b) is referred to as ''FO mode'' or ''FO orientation''. Some researchers refer to it as ''active layer facing feed solution'' (AL-FS). This is the most common orientation for testing of FO applications. The orientation in which the active layer is in contact with the draw solution (Fig. 5c) is referred to as ''PRO mode'', ''PRO orientation'', or ''active layer facing draw solution'' (AL-DS). In PRO energy recovery application the active layer must face the draw solution where hydraulic pressure is applied, so that the support layer can provide proper mechanical strength. It is important to note that in many laboratory studies that test ODMP membrane in PRO orientation, the transmembrane hydraulic pressure is minimal and approaches zero.

6.1 Water and solute fluxes in ODMPs

The classical solution-diffusion model coupled with diffusion–convection is generally used to explain solute and water transport behaviour in semipermeable membranes. As shown in Fig. 4(b), the water flux (J_w) (m s^{-1}) across the membrane in FO and PRO is in the ideal case a linear function of the applied hydraulic pressure (ΔP) and depends on the osmotic pressure difference (constant) across the membrane:

$$J_w = A(\Delta\pi - \Delta P) \quad (1)$$

where A is the water permeability constant (m s^{-1} Pa^{-1}), which is an intrinsic characteristic of the membrane. In RO, the components in the parenthesis in eqn (1) are reversed (*i.e.*, $\Delta P - \Delta\pi$). The power generated by a PRO system is expressed by ref. 23

$$W = J_w\Delta P = A(\Delta\pi - \Delta P)\Delta P \quad (2)$$

The power generated by PRO is a parabolic function of ΔP in which the maximum value is at $\Delta P = \Delta\pi/2$. Thus, the maximum theoretical gross power that can be generated by PRO ($W_{max} = A\Delta\pi^2/4$) is proportional to the water permeability constant and the square of the osmotic pressure difference.

The salt flux (J_s) in ODMPs is defined by

$$-J_s = B(\Delta C) \quad (3)$$

where B is the salt permeability coefficient (m s^{-1}) and ΔC is the concentration difference across the membrane selective layer. The salt permeability coefficient B of membranes can also be determined using eqn (4) and (5):

$$B = \frac{A(1-R)(\Delta P - \Delta\pi)}{R} \quad (4)$$

$$R = 1 - \frac{C_p}{C_f} \quad (5)$$

where R is the salt rejection of the membrane (*i.e.*, the fraction of salts retained in the feed solution), and C_p and C_f are the salt concentration in the permeate and in the feed solution, respectively.

While these equations describe solute and solvent fluxes through semipermeable membranes, by themselves they cannot describe mass transport in ODMP because of concentration polarization phenomena that occur inside and outside the membrane and have to be considered when describing water and salt fluxes through the membrane.

6.2 Concentration polarization

Concentration polarization is a common phenomenon in membrane processes and appears when the concentration of solution at the membrane–feed interface is higher than that of the bulk solution due to depletion of water from the boundary layer.[105] Concentration polarization is in general more severe in ODMPs compared to other membrane processes. Moreover, there are two types of concentration polarization in FO and PRO, external and internal concentration polarization. The concentration polarization developed at the membrane–liquid interface (*i.e.*, external concentration polarization (ECP)), and that developed inside the membrane support structure (*i.e.*, internal concentration polarization (ICP)) are illustrated in Fig. 5. In FO and PRO, the solute flux is in the opposite direction to the water flux, making them unique from pressure-driven membrane processes (Fig. 4). When RO-type membranes

are used in an ODMP, ICP develops in the porous support layer due to depletion of salts (dilutive ICP (DICP) when operating in FO orientation) or concentration of salts in the porous support layer (concentrative ICP (CICP) when operating in PRO orientation). The presence of ICP has a significant impact on the effective osmotic pressure difference ($\Delta\pi_{eff}$) across the membrane, which can cause high reduction in the productivity (water flux) in FO and PRO.

In ODMPs ECP occurs on both sides of the membrane at the interface of the bulk feed and draw solutions. During operation the concentration of solutes at the membrane–feed interface is higher than in the bulk feed solution due to the retention of salt by the membrane. This is referred to as concentrative ECP (CECP). On the draw solution side, the solution at the membrane–draw solution interface becomes diluted due to diffusion of water into the draw solution, thus the ECP on the draw solution side is referred to as dilutive ECP (DECP). The ECP can be reduced by minimizing the thickness of the boundary layer at the solution/membrane interface by enhancement of mixing or flow conditions.[107]

Lee *et al.* (1981) were the first to explain ICP in ODMPs and developed models that take into consideration the salt leakage of membranes to predict the performance of membranes in PRO.[23] Due to the reduction of the osmotic driving force by the concentration polarization effects, the term *effective osmotic pressure* was introduced and was denoted $\Delta\pi_{eff}$. Thus, a more accurate description of water flux was proposed:

$$J_w = A(\Delta\pi_{eff} - \Delta P) \tag{6}$$

It is worth noting that the term reflection coefficient (σ), which refers to the ratio of $\Delta\pi_{eff}$ to the actual osmotic pressure difference ($\Delta\pi_{eff} = \sigma\Delta\pi$), is more common in a pressure driven process.[23] In the porous substrate (support layer), the salt flux is the result of diffusion following the concentration gradient, which is in the opposite direction to the convective flow of salts with water flow through the membrane substrate. Thus, J_s can also be written as a function of diffusion and convection – the first and second terms in eqn (7), respectively:

$$-J_s = D\varepsilon\frac{dC(x)}{dx} - J_w C(x) \tag{7}$$

where D is the salt diffusion coefficient ($m^2\ s^{-1}$) and ε is the substrate porosity. Here, the salt flux (with negative sign) is in the opposite direction of the water flux. Therefore,

$$B(C_{D,m} - C_{F,i}) = D\varepsilon\frac{dC(x)}{dx} - J_w C(x) \tag{8}$$

where $C_{F,i}$ and $C_{D,m}$ are the salt concentration of the feed solution inside the substrate near the selective layer and the concentration of the draw solution near the membrane surface, respectively. Under the boundary conditions of $C(x) = C_{F,m}$ at $x = 0$ and $C(x) = C_{F,i}$ at $x = \tau t$, where τ and t are membrane tortuosity and thickness, eqn (8) can be resolved to

$$\frac{C_{F,i}}{C_{D,m}} = \frac{B[\exp(J_w K) - 1] + J_w\frac{C_{F,m}}{C_{D,m}}\exp(J_w K)}{B[\exp(J_w K) - 1] + J_w} \tag{9}$$

where K is the solute resistivity to salt transport in the porous substrate, which is defined as a function of the structural parameter S and the diffusion coefficient D,

$$K = \frac{t\tau}{D\varepsilon} = \frac{S}{D} \tag{10}$$

The ratio of salt concentration is assumed to be approximately equal to the ratio of osmotic pressure:

$$\frac{\Delta\pi_{eff}}{\Delta\pi} = \frac{\pi_{D,m} - \pi_{F,i}}{\pi_{D,m} - \pi_{F,m}} \cong \frac{C_{D,m} - C_{F,i}}{C_{D,m} - C_{F,m}} = \left(\frac{1}{1 - \frac{C_{F,b}}{C_{D,m}}}\right)\left(\frac{1 - \frac{C_{F,b}}{C_{D,m}}\exp(J_w K)}{\frac{B}{J_w}[\exp(J_w K) - 1] + 1}\right) \tag{11}$$

By substituting $\Delta\pi_{eff}$ from eqn (11) into eqn (6), the water flux can be rewritten as

$$J_w = A\left[\left(\frac{C_{D,m} - C_{F,m}\exp(J_w K)}{\frac{B}{J_w}[\exp(J_w K) - 1] + 1}\right) - \Delta P\right] \tag{12}$$

Once proper flow or stirring conditions are applied, the ECP effect at the feed side of the membrane is suppressed. The concentration at the membrane interface is thus equal to the bulk solution; $C_{D,m} = C_{D,b}$ and $C_{F,m} = C_{F,b}$. Therefore,

$$J_w = A\left[\left(\frac{C_{D,b} - C_{F,b}\exp(J_w K)}{\frac{B}{J_w}[\exp(J_w K) - 1] + 1}\right) - \Delta P\right] \tag{13}$$

There is no effective direct measurement of the structural parameter (eqn (10)). However, K can be estimated by measuring the flux when no hydraulic pressure is applied and pure water is used as a feed:

$$K = \frac{1}{J_w}\ln\left(\frac{A\pi_{D,m} - J_w}{B} + 1\right) \tag{14}$$

Loeb *et al.* (1997) derived the equation for K for membranes in both PRO and FO configurations.[21] This equation was widely used as a reference under the assumption of ideal solutions.

$$K = \left(\frac{1}{J_w}\right)\ln\frac{B + A\pi_{D,m} - J_w}{B + A\pi_{F,b}} \tag{15}$$

for PRO mode and

$$K = \left(\frac{1}{J_w}\right)\ln\frac{B + A\pi_{D,b}}{B + J_w + A\pi_{F,m}} \tag{16}$$

for FO mode

With better membranes and knowledge developed for ODMPs, recent intensive research proposed more accurate models to explain the flux behaviour.[20,31,36,37,65,108–110]

6.3 Phenomena governing water flux and power density

6.3.1 External concentration polarization (ECP). McCutcheon *et al.* intensively investigated the correlation between flux and concentration polarization.[20,36,111,112] Their models solved the limitation of earlier models that ignored ECP. The ECP moduli were developed based on the boundary layer film theory.[20,113]

$$\frac{\pi_{F,m}}{\pi_{F,b}} = \exp\left(\frac{J_w}{k}\right) \tag{17}$$

for CECP in FO mode and

$$\frac{\pi_{D,m}}{\pi_{D,b}} = \exp\left(-\frac{J_w}{k}\right) \tag{18}$$

for DECP in PRO mode

where k is the mass transfer coefficient in the flow channel, and is calculated using the Sherwood number (Sh):

$$k = \frac{\mathrm{Sh}D}{d_h} \tag{19}$$

where D is the diffusion coefficient of the solute in draw or feed solution and d_h is the hydraulic diameter of the flow channel. It is worth noting that the ratio of osmotic pressure at the membrane surface to that in the bulk solution is assumed to be equivalent to the ratio of concentrations. This is reasonable for relatively dilute solutions following Van't Hoff's equation. Common formulas used in calculating the Sherwood number for different flow regimes in a rectangular channel include:

$$\mathrm{Sh} = 1.85\left(\mathrm{Re}\,\mathrm{Sc}\frac{d_h}{L}\right)^{0.33}$$

(laminar flow; Re $\leq$ 2100); and

$$\mathrm{Sh} = 0.04\ \mathrm{Re}^{0.75}\mathrm{Sc}^{0.33}$$

(turbulent flow; Re $\leq$ 2100)

where Re is the Reynolds number, Sc the Schmidt number, and L is the length of the flow channel.

From eqn (17) and (18), it is clear that the ECP moduli are strongly related to mass transfer coefficient and the hydrodynamic conditions of the system. Different models to calculate k and Sh for different flow conditions and membrane modules (*e.g.*, spiral wound, flat-frame, or tubular module) have also been developed and can be found elsewhere.[20,35–37,114–119]

6.3.2 Internal concentration polarization (ICP). The corrections for the DICP and CICP are given by ref. 20 and 36

$$\frac{\pi_{D,i}}{\pi_{D,b}} = \exp(-J_w K) \tag{20}$$

DICP in FO mode and

$$\frac{\pi_{F,i}}{\pi_{F,b}} = \exp(J_w K) \tag{21}$$

CICP in PRO mode

For simplicity, the applied hydraulic pressure is omitted in the following equations. By incorporating the correction factors (eqn (17) and (20)) into eqn (6), the flux equation in FO mode becomes

$$\begin{aligned} J_w &= A(\Delta\pi_{eff}) = A\left(\pi_{D,i} - \pi_{F,m}\right) \\ &= A\left[\pi_{D,b}\exp(-J_w K) - \Delta\pi_{F,b}\exp\left(\frac{J_w}{k}\right)\right] \end{aligned} \tag{22}$$

And when incorporating the correction factors (eqn (18) and (21)) into eqn (6), the flux equation in PRO mode becomes

$$\begin{aligned} J_w &= A(\Delta\pi_{eff}) = A\left(\pi_{D,m} - \pi_{F,i}\right) \\ &= A\left[\pi_{D,b}\exp\left(-\frac{J_w}{k}\right) - \Delta\pi_{F,b}\exp(J_w K)\right] \end{aligned} \tag{23}$$

These equations assume that there is no ECP at the porous support side. Water and solute can freely transport through the porous support layer and thus the concentration at the support interface is equal to that in the bulk solution.[112] It is also worth noting that the moduli for ECP and ICP are derived under the conditions of a very high salt rejection membrane ($\sigma \approx 1$). Therefore, salt permeability and salt reverse flux are negligible (*i.e.*, $B \approx 0$). With newly developed membranes specially designed for ODMPs, high water flux can be achieved and thus the ECP cannot be ignored anymore.

Achilli *et al.* applied the ECP moduli to Lee's models and found that the extended model can explain the flux behaviour of osmotic membranes better than the original models.[114] Later on, Yip *et al.* combined ECP, ICP, and reverse salt flux into their flux model (as shown in eqn (24)) to predict the performance of their membranes in the PRO process.[120]

$$J_w = A\left[\frac{\pi_{D,b}\exp\left(-\frac{J_w}{k}\right) - \Delta\pi_{F,b}\exp(J_w K)}{1 + \frac{B}{J_w}\left[\exp(J_w K) - \exp\left(-\frac{J_w}{k}\right)\right]}\right] \tag{24}$$

6.3.3 Reverse solute flux. To better understand the ICP in ODMPs and further improve the process, it is important to understand the fundamentals of solute transport through an osmotic membrane. Recently, more attention has been paid to develop models explaining solute fluxes in ODMPs.[16,118,121–127] Reverse solute fluxes in the opposite direction of water flux in ODMPs not only decrease the osmotic pressure driving force of the process and the need for replenishing draw solution, but may also have a negative impact on downstream processes in some applications.[123] Simultaneous solute flux from the feed into the draw solution might also exacerbate the situation.[109,122]

The flow of salt from the draw solution into the feed solution involves transport across three regions, as shown in Fig. 6. These include the porous support layer, the dense selective layer and the boundary layer. The solute transport in the boundary layer and the support layer is governed by both diffusion and convection, while the transport in the dense

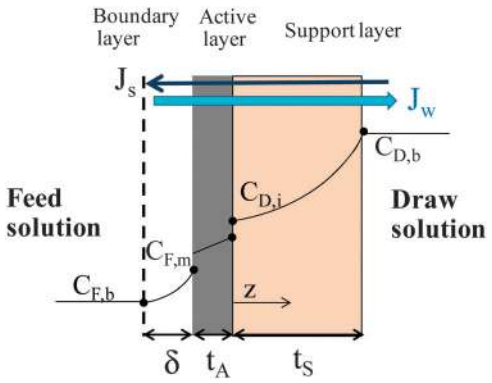

Fig. 6 Profiles of the solute concentration across an asymmetric membrane. The solute permeates from the higher salt concentration through the membrane support layer with thickness t_S, the dense selective skin with thickness t_A, and through the boundary layer with thickness δ to the feed bulk solution (adapted from Yong *et al.*).[128]

selective layer is controlled only by diffusion.[123] The solute flux across the three layers is expressed as

$$J_s = \frac{J_w\left(C_{F,b}\exp\left(Pe^s + Pe^\delta\right) - C_{D,b}\right)}{(B\exp(Pe^s) + J_w)\exp(Pe^s) - B} \quad (25)$$

where

$$Pe^s = J_w\frac{t_s\tau}{\varepsilon D} = J_w\frac{S}{D} = J_wK \quad (26)$$

$$Pe^\delta = \frac{J_w}{k} \quad (27)$$

Here, Pe^s is the Peclet number in the support layer and Pe^δ is the Peclet number of the boundary layer. The reverse solute flux in eqn (25) was derived in terms that can be experimentally measured. The detailed derivation can be found elsewhere.[106,128] Interestingly, the physicochemical properties of the draw solute play as a crucial a role as the membrane properties in reverse and forward salt fluxes. Hancock *et al.* investigated several factors that influence reverse salt fluxes. The size, viscosity, and diffusion coefficient of the solutes all were found to have an impact on solute flux.[122,123] Moreover, the reverse salt transport can accelerate concentration polarization and fouling, which further reduced water flux and membrane performance.

6.3.4 Water/salt selectivity in ODMPs. The ratio of the water flux to the reverse solute flux is defined as the volume of water produced per mass of draw solute lost. The relationship between this term and membrane and process properties was established independently by two research groups.[106,128]

$$\frac{J_w}{J_s} = \frac{A}{B}\beta R_g T \quad (28)$$

where β is the van't Hoff coefficient, R_g the ideal gas constant, and T the absolute temperature. Interestingly, the reverse salt flux selectivity (J_w/J_s) is independent of structural parameters but depends on the water permeability (A) and salt permeability (B) through the membrane, which are related to the selective layer of the membrane only.[122] In addition, it does not change with concentration of the draw solution and operating conditions.[106,122] Therefore, a draw solution that can generate high osmotic pressure (βRT) would be obviously preferred.[106]

Hancock *et al.* investigated the bidirectional mass transport of solutes in two different membranes, cellulose acetate membranes and polyamide thin film composite membranes, with different electrolyte solutions and various operating conditions.[122,123] Even though the rate of reverse salt flux and water flux changed dramatically with operation conditions, and types of solute used, the water–salt selectivity (J_w/J_s) of a given membrane remained relatively constant under similar osmotic driving force.

The above discussion was relevant to the FO process without any hydraulic pressure applied. She *et al.* investigated the effects of operating conditions on the reverse solute diffusion and the specific solute flux (J_s/J_w) in the PRO process.[126] The ratio of J_s/J_w was found to increase with hydraulic pressure applied, implying that eqn (25) underestimates reverse salt flux under specific operating conditions, and a modified equation of specific reverse solute flux for PRO was proposed:

$$\frac{J_s}{J_w} = \frac{B}{A\beta R_g T}\left(1 - \frac{A\Delta P}{J_w}\right) \quad (29)$$

The increase in the specific reverse solute flux with applied pressure was attributed to the deformation of the commercial membranes used. At high applied pressure, polymer chains of the membrane selective layer may be stretched and pores got enlarged, resulting in the reduced solute rejection. In summary, increased water flux and operating pressure in PRO will always be accompanied by an undesired increase in reverse solute flux. Membranes with better selectivity (high A/B) are thus greatly desired and should be developed.

6.3.5 Influence of membrane properties and operating conditions. The influence of type and concentrations of feed and draw solutions on both ECP and ICP was investigated with commercial osmotic membranes (CTA, HTI) tested in different orientations, including in PRO and FO modes.[20,33,36] For membranes tested in PRO mode, where the membrane active layer contacts the draw solution and the porous support contacts the deionized water, increased draw solution concentrations (osmotic pressure difference) resulted in water fluxes close to those obtained under RO experiment (Fig. 7a). However, a slight deviation at a higher driving force (draw solution concentrations) was observed.[33] This trend was attributed to ECP only, because the reverse salt diffusion across the selective skin layer to the porous support was negligible for the commercial osmotic membrane with high salt retention.[20,114] Moreover, sizes and diffusivity of different solutes had no influence in this case.

For membranes tested in FO orientation, the physicochemical properties of solutes, including sizes, viscosity, and concentration, had a strong impact on water flux. Non-linear flux behaviour was observed and it was found to be more severe with larger hydrated solute sizes and lower diffusivity (Fig. 7b). In FO orientation, the solutes in the draw solution have to diffuse in the porous support to the selective layer and reach the state that can draw water from the feed. Therefore, bulkier and

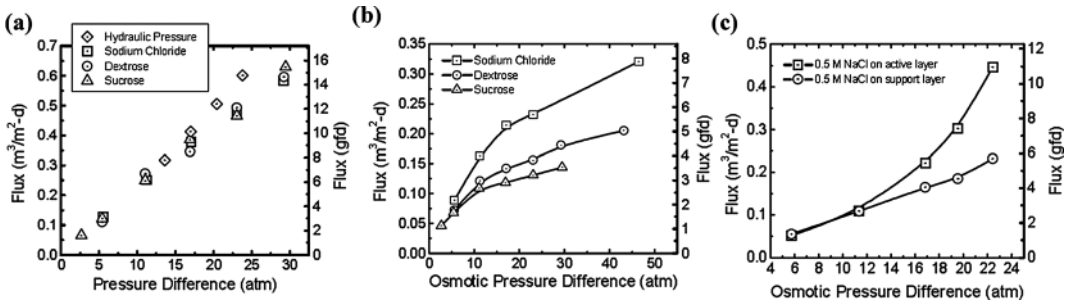

Fig. 7 Water flux as a function of driving force. The experiments were run with three different solutes in the draw solutions – NaCl, dextrose, and sucrose – and DI water as feed solution. Commercial osmotic membranes were orientated in (a) PRO mode and (b) FO mode. (c) Water flux for 0.5 mol L^{-1} NaCl draw solution and various NaCl concentrations in the feed. Reprinted with permission from ref. 33. Copyright 2008, Elsevier.

slower diffusing molecules caused more severe DICP in this configuration. However, when the feed stream contains solutes like in real practical environments, membranes in PRO mode suffer severely from ICP.

Compared to the same osmotic pressure difference, when the feed solutions contained low concentration of the solute, different flux behaviours were observed (Fig. 7c). Water flux in PRO mode dramatically declined with the presence of solutes in the feed solution, indicating severe CICP. As the ECP and ICP are functions of water flux, the increased feed concentration resulted in lower flux and thus less concentration polarization. The modulus of CICP was found to increase (further away from the ideal case) with water flux.[114] On the other hand, the flux behaviour in FO mode became more linear (the flux was still much lower than the ideal case). The addition of solutes into the feed solution did not contribute directly to the increase in DICP in the porous support layer on the draw solution side of the membrane in FO configuration, but to the driving force and thus the water flux through the membrane.[20,36] The increased feed concentration decreased water flux and consequently ECP and ICP were also reduced. Though the aim of the diminishing concentration polarization is to increase water flux and efficiency of the system, the increase in flux by itself is self-limiting.[20,36,111,112,129] This is because both ECP and ICP are a function of flux, as mentioned earlier. The higher the flux, the more pronounced the concentration polarization effects. The strategy of using high draw solution concentrations to increase driving force and flux is thus restricted to a certain degree. The influence of feed concentration on water flux and concentration polarization moduli is summarized in Table 3.

It is worth noting that the trends in Table 3 were taken from McCutcheon and Elimelech data where HTI commercial membranes were tested in FO orientation with a fixed 1.5 mol L^{-1} NaCl draw solution and various NaCl feed concentrations ranging from 0 to 1.0 mol L^{-1}.[36] The ECP at the porous support layer was assumed to be negligible. The solute resistivity K and the moduli for ICP and ECP were estimated from their developed models (eqn (17) through (21)).

The flow velocity parallel to the membrane surface is directly related to mass transfer near the feed–membrane interface. Gruber *et al.* used computational fluid dynamics (CFD) to investigate the influence of various hydrodynamic flow conditions and feed concentration on ECP and membrane flux. The assumption of ignored ECP at the porous support side in earlier work was also verified in an FO configuration.[130] Solute resistivity K, in accordance with Lee's models, is a function of the structural parameter S and of the diffusion coefficient of the solute, D. There is no effective means to directly measure K; instead, K is estimated from water flux, which varies depending on various operating conditions. Thus, K also depends on mass transfer coefficients and can therefore be influenced by flow conditions (Fig. 8a). The value of K declines with increasing liquid flow rate due to better hydrodynamic conditions and enhanced mass transfer. Osmotic pressure differences based on solute fraction profiles across the membrane were stimulated and the results are shown in Fig. 8b and c. Increased draw

Table 3 Correlation between feed concentration, water flux, ICP, and ECP modulus[36]

	Concentration					Modulus				
Membrane orientation	Draw solution	Feed solution	$\Delta\pi$	Flux	K	CECP	DECP	CICP	DICP	$\Delta\pi_{eff}/\Delta\pi$
FO mode	Fixed	↓	↑	↑	↑	↑ 1	—	—	↓ 1	1 ↑
PRO mode	Fixed	↓	↑	↑	↓	—	↓ 1	↑ 1	—	1 ↑

Remarks: arrows points to the higher values. (1) indicates the value in the ideal case where there is no influence from concentration polarization.

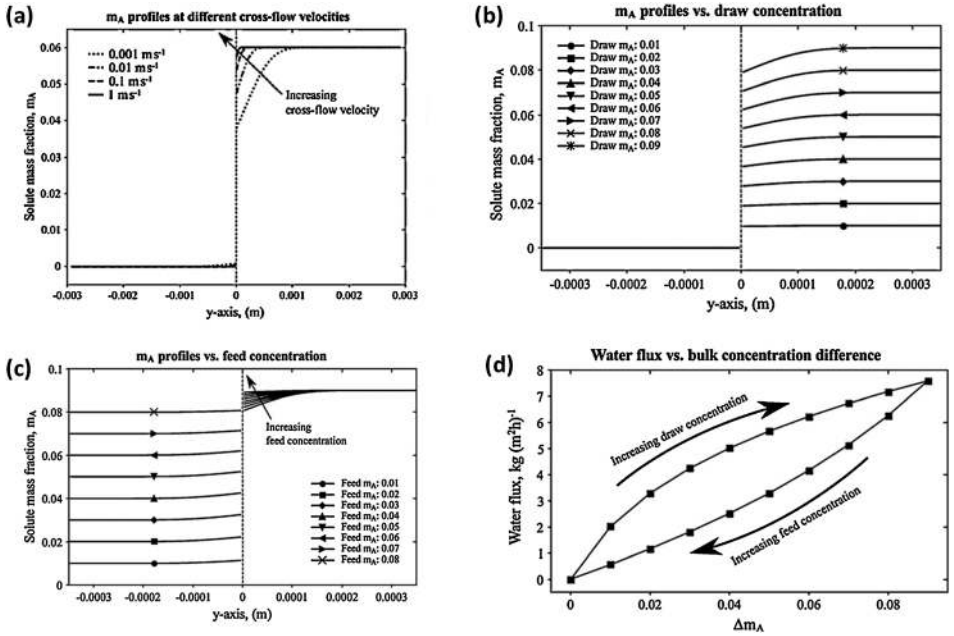

Fig. 8 (a) Solute mass fraction profiles along the *y*-axis at the centre of membranes resulting from different cross-flow velocities. Simulation results at different bulk draw–feed concentrations; (b) increasing draw solution concentrations/DI water feed; (c) constant draw solution concentration/increasing feed concentrations; and (d) water flux corresponding to the simulation conditions in (b) and (c). Reprinted with permission from ref. 130. Copyright 2011, Elsevier.

Table 4 Influence of operating conditions and intrinsic membrane parameters on membrane performance in ODMPs

Parameter	Effect
Operating conditions	
(1) Membrane orientation	The degree of ICP, fouling, and flux stability depend highly on the membrane orientation in specific operating conditions.[33,110,131,132]
(2) Solution concentration	Influences the magnitude of ECP and ICP, depending on the membrane orientation. In general, the lower the solution concentration, the lower the CP effects, but also the lower the flux.[114,132,133]
Draw solution	Increased concentration causes increased driving force but also increases both ICP and ECP.[106,114] Though water flux is enhanced, the reverse solute flux also increases and thus causes more severe ICP effects.[125,126,128]
Feed solution	Increased concentration will enhance CICP in PRO configuration. In FO configuration, the increased feed concentration will reduce the flux and degree of ECP and DICP.[114]
(3) Flow rate of feed and draw solution	Increasing flow rate lower possible ECP effects due to the better hydraulic conditions and might thus increase fluxes.[118,134]
(4) Temperature	Increased temperature increases mass transfer and diffusion rates of both solvent and solute.[126,135] As ECP and ICP are proportional to the water flux, it only has a small impact on the overall performance.[36]
Membrane properties	
(5) Intrinsic membrane parameters	
A	To obtain high water flux in FO or a high power density in PRO, membranes should possess high water permeability A.
B	The salt permeability B depends on intrinsic properties of the dense top-layer. This parameter needs to be low enough to suppress the reverse salt flux through the support layer.[22] Note: A and B need to be optimized, since most membranes possess opposite trends of these two properties.
(6) Membrane structural parameters	
$S = \frac{t\tau}{\varepsilon}$	Regarded as the characteristic distance the solute needs to diffuse through. As large S values lead to severe ICP, relatively thin membranes with low tortuosity and high porosity are preferred.[22] Ideally <0.5 mm.[136]
$K = \frac{S}{D}$	Closely related to ICP. The higher the K value, the stronger the effect of ICP and thus the lower the membrane flux.[20,36]

solution concentrations result in increased ECP at the porous support side. With the addition of more solutes in the feed, the ECP on the feed side slightly increased and became less severe with increased feed concentration. The increased feed concentrations also induced reduction in the water flux, which in turn reduced the severity of ECP and ICP. The water fluxes in Fig. 8d show non-linear behaviour with hysteresis, attributed to the significant impact of CP. Though the better flow conditions

can reduce ECP to a certain extent, ECP on the support side should not be ignored if the water flux in the process is high.

The role of several operating parameters and intrinsic membrane properties in optimizing the performance of ODMPs is summarized in Table 4.

Both fundamental studies and computational modelling point to the conclusion that it is vital to improve both the structure and separation properties of ODMP membranes. It has been proved that by means of controlling operating conditions alone, the performance of ODMPs can only slightly be enhanced.[36,112,129] Recent improvements in the development of ODMP membranes are discussed in detail in Section 8.

7. Fouling in ODMP

Fouling can be classified into four major types,[76,137,138] including colloidal fouling from particle deposition; inorganic fouling due to crystallization/scaling of sparingly soluble salts; organic fouling caused by organic compounds such as alginate, protein, and natural organic matters; and biofouling due to deposition/adhesion of microorganisms.

Fouling in membrane processes is a complex problem, affected by several factors, including solution chemistry and level of pre-treatment, membrane properties, and operating conditions. To avoid severe membrane fouling, it is important to avoid operating above the critical flux. At a higher water flux, the fouling is promoted by (1) greater hydrodynamic force, dragging the foulants toward the membrane surface, and (2) more severe concentration polarization (and more foulant concentration near membrane surface).[110]

Several model foulants such as proteins, humic acids, alginates, and silicates have been used to study the fouling in FO membranes.[77,78,139] Like in pressure-driven membrane processes, fouling in ODMPs is governed mainly by chemical and hydrodynamic interactions.[139] However, it was found that the mechanism of fouling and flux decline in FO is more complicated compared to the fouling in a pressure-driven membrane process, mainly due to the coupled effects of ICP and reverse salt flux.[110]

Cellulose acetate (CA) and polyamide (PA) thin film composites were used for studying the role of membrane materials in alginate fouling, gypsum scaling, and cleaning.[77,78] The results suggest that the PA membrane is more susceptible to foulant adsorption due to its more hydrophobic characteristics and increased surface heterogeneity. In addition, gypsum scaling on the PA membrane was found to be more severe compared to scaling on the CA membrane. Because the PA membrane surface contains negatively charged carboxyl groups that can form complexes with Ca^{2+} ions, gypsum prenucleation clusters can be initiated that further develop to form amorphous gypsum nanoparticles and polycrystals.[78] On the other hand, dominant surface hydroxyl functional groups on the CA membranes do not have interactions with Ca^{2+} or SO_4^{2-} ions.

Though alginate fouling and gypsum scaling rates in ODMPs and RO are similar, the hydraulic pressure applied makes the structure of their fouled/scaled layers different, and thus, different cleaning procedures are required. The alginate fouling in ODMPs was found to be almost fully reversible. More than 98% water flux recovery could be obtained after water rinsing,[77] which is much higher than that commonly observed in RO.[77] This was attributed to the less compact fouled layer due to the absence of hydraulic pressure in FO. Thus, in many

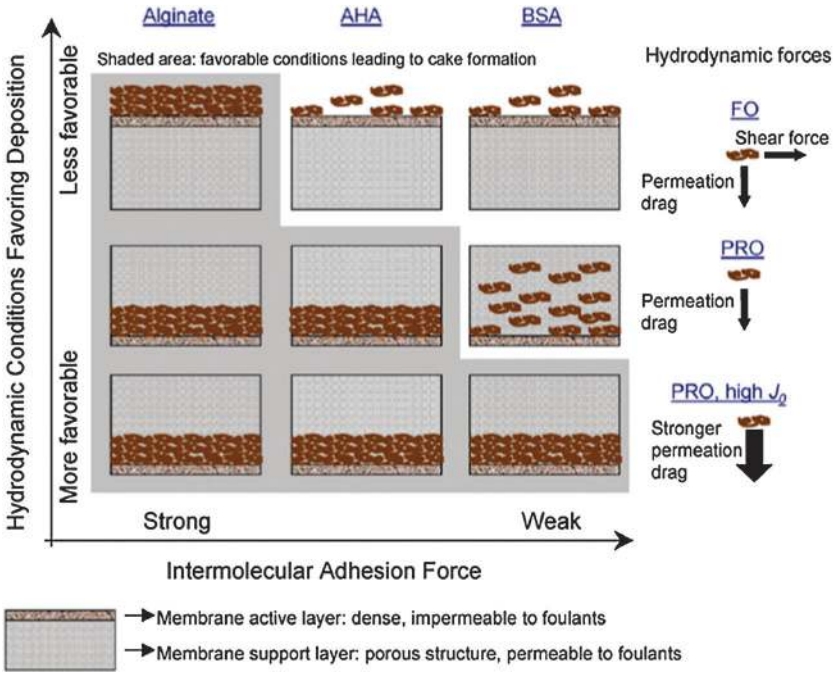

Fig. 9 Schematic illustration of the coupled influence of intermolecular adhesion and hydrodynamic force on membrane fouling by alginate and humic acid (bovine serum albumin-BSA and Aldrich humic acid-AHA). Reprinted with permission from ref. 139. Copyright 2008, Elsevier.

applications chemical cleaning might not be required for ODMP membranes. Results from investigation of combined fouling of alginate and gypsum were also recently reported.[76] The flux decline due to the combined fouling was much more dramatic compared to the individual fouling, implying synergistic effects between alginate fouling and gypsum fouling. It was suggested that alginate molecules shorten the nucleation time by acting as the nuclei in gypsum crystal growth and accelerating the scaling rate of gypsum. In addition, water flux through the gypsum–alginate fouled membrane could not be fully recovered after cleaning with pure water. Alternative cleaning procedures were required.

Tang *et al.* systematically investigated humic acid fouling behavior in FO and PRO mode.[110] Membranes in PRO mode could generally generate a higher water flux at the same osmotic pressure compared to the membrane in FO mode due to its less severe ICP. However, PRO is prone to fouling and less stable fluxes.[110,140] The porous support layer of the membrane in PRO mode is in contact with foulants in the feed solution and often gets clogged by the foulants. This internal clogging reduces the structure parameter and thus mass transfer through the PRO membrane, resulting in enhanced ICP and drastic flux decline.[110] Moreover, foulants of films deposited inside the pores of PRO membranes are hard to remove. Mi and Elimelech reported a similar effect of membrane orientation on membrane fouling and suggested that shear velocity was vanished and blocked by the pore once the membrane was orientated in PRO mode.[139] The general correlation between the coupled intermolecular adhesion force and the hydrodynamic conditions on membrane fouling in ODMPs (both FO and PRO modes) were proposed by Mi and Elemilech as illustrated in Fig. 9.[139]

Wang *et al.* applied a direct microscopic observation to study the fouling of the FO process in two configurations.[141] This study revealed the morphology of the fouling film on the membrane surface. Foulants seemed to deposit more on the rougher surface region adjacent to the embedded mesh support of the commercial CTA HTI membranes. In addition, the lower fouling propensity of the membrane in FO mode could be attributed to the smoother surface and the lower initial flux that this configuration could create at the same osmotic pressure. Also, the effect of the spacer used was investigated. It was found that the spacer enhanced mass transfer and reduced the rate of flux decline. At a similar initial water flux, membranes in FO mode demonstrated superior flux stability against fouling.[110]

So far, most fouling studies in ODMPs have been based on simple foulants and individual foulant tests. Only a few studies conduct the test under real feed/seawater conditions.[142] A better understanding of fouling in ODMPs and the development of suitable treatment and cleaning procedures are still needed.

8. Osmotic membrane developments

With the recently renewed interest in FO and PRO, the development of membranes specific for ODMPs is now accelerating. There are now three commercial osmotic membranes available in the market, two from Hydration Technology Innovations (HTI) and one from Oasys Water. Two major approaches have been applied to develop better membranes for ODMPs. The first strategy is to modify available commercial membranes.[111,143] This approach is considered simple and effective to some extent, attempting to use existing membranes for cost effective purposes, because only a modification step has to be added to the existing membrane manufacturing process. However, the enhanced properties are still limited, being restricted by the inherent properties of the parent membranes that were developed for other processes. The second strategy involves the development of new membranes specifically designed for ODMPs, with the potential to overcome the current barriers of ICP and other mechanical and chemical limitations.

8.1 Modification of available NF or RO membranes to ODMP membranes

Ideal membranes for RO have high water flux and good salt rejection, good mechanical strength, and high chemical stability. Existing commercial RO membranes have either asymmetric structure or thin film composite cross-section consisting of a dense top-layer for selectivity purpose and a thick porous sub-layer for mechanical support.[144,145] The commercial high-pressure membranes (*e.g.*, RO and NF) are inadequate for ODMPs due to the severe ICP inside the support layer.[23,111,120,143,146–148] Current strategies to modify commercial RO and NF membranes for use in PRO and FO are illustrated in Fig. 10.

The membranes can be simply modified by removing the backing support layer of the RO or NF membranes. In FO, and to some extent in PRO, the operating pressures are lower than in RO and therefore less mechanical support is required for the membrane. By removing the backing support layer, the water flux of the membranes can be substantially improved by a factor of 5 in FO.[111] This is due to the reduced salt passage resistivity and low ICP. Although the FO water flux through RO membranes can be remarkably improved after the removal of backing fabrics, much care has to be exercised to avoid mechanical damage to the membrane.

In another approach, the pore wettability can be improved. Unlike in RO where pore wettability does not play a significant role, the presence of un-wetted areas or air gaps in the membrane pores in ODMPs can block the water flux and dramatically exacerbate ICP.[111] Polydopamine (PDA) is a highly hydrophilic polymer widely used in coatings to improve wettability, flux, and fouling resistance.[143,149–151] Recently, PDA-modified RO membranes for FO demonstrated a ten-fold increase in water flux compared to the parent membranes.[143] The main risk associated with such membrane modification is that it can clog some small pores of the membranes, which might result in declined water fluxes.[143]

8.2 Currently developed osmotic membranes

Increased interest in ODMPs resulted in a recent acceleration of membrane research and development. A review of the literature (Table 5) reveals that many membranes for ODMP with a wide variety of characteristics are being developed. However, due to lack

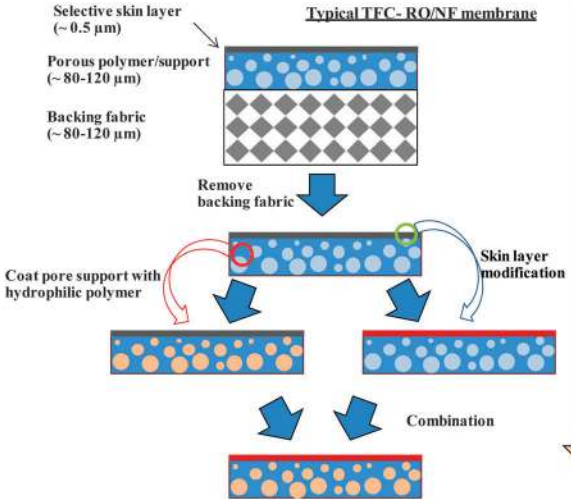

	Modification effects
Pristine RO/NF membrane	Severe ICP in porous support
Backing support removal	Reduced pathway for water and salt flux. The water flux can be improved 5-10 folds.
Skin layer	Optimization of B/A ratio leads to improved water flux and reduced ICP from the reverse salt flux
Hydrophilicity of the support	Increased support hydrophilicity and ensured wettability of pores can enhance flux up to 10 times.
Surface and structural support modification	Effective modification of both chemical property of support and skin layer would lead to significant flux and performance improvement. However, it is difficult to improve properties of skin and support layers separately. This area still needs to be further explored.

Fig. 10 Modification procedures for commercial RO and NF membranes.

of a standard procedure to characterize these new membranes, it is difficult to compare their performance. Different research studies apply different testing conditions that make it very difficult to evaluate the results. A recent publication suggested a standard method and demonstrated it through comparison between three commercial ODMP membranes.[152] The influence of testing conditions on membrane properties such as *A*, *B*, and fluxes of a membrane could be easily noticed from the reports of the same commercial membranes. Under different testing conditions, the results were diverse. In order to fairly compare the performance of membranes in the literature, the normalized fluxes and power density values that take into account the differences in driving force ($\Delta\pi$) and the applied hydraulic pressure were introduced in Table 5.

Increasing the water flux by minimizing ICP effects is currently the main focus of new ODMP membrane development. Because ICP occurs inside the porous support layer of the membranes, a membrane structure or membrane chemistry needs to be designed to favour the transport of water and solutes. FO and PRO membranes have usually been redesigned from the materials that have been reported to give good performance in RO or NF. An ideal ODMP membrane has to be ultrathin with minimal resistivity to permeating molecules. Because there is no technique that can prepare defect-free, stand-alone ultrathin films, membranes are generally prepared in a much thicker form that can withstand the operating conditions in either symmetric or asymmetric configuration. And because dense symmetric membranes show very poor water flux, ultrathin selective layers are commonly formed on a much thicker porous support layer to combine mechanical strength with good flux. Most commercial membranes are thus asymmetric. The barrier layer and support are either made of the same materials or commonly prepared separately in a thin-film-composite (TFC) membrane structure.

8.2.1 Asymmetric membranes. Asymmetric membranes are typically prepared *via* the phase inversion method.[172] Most asymmetric membranes for aqueous applications are cellulose acetate (CA) based membranes. CA is a relatively low cost polymer and has been used in the fabrication of RO membranes for several decades.[153,173] Due to its hydrophilic properties, CA resists fouling relatively well and in membranes can achieve good water flux.[153,174] In addition, CA membranes possess good resistance to chlorine and other oxidants commonly used in the pre-treatment of feed water and cleaning of the membrane.[173] CA is in fact the common name used to describe CA polymers with a different degree of acetylation. Most CA based membranes are either made from cellulose diacetate (CDA), cellulose triacetate (CTA), their combination, or from blends with other polymers.[173,175–178] The blends are aimed to deal with the disadvantages of CA, including low thermal and mechanical stabilities.

Sairam *et al.* reported a wide range of asymmetric membranes prepared by casting polymer solutions of CA and CTA on a woven fabric, adapting the large-scale synthesis procedure reported in the HTI patents.[155,156] The effect of dope composition and various pore-forming agents such as lactic acid, maleic acid, and zinc chloride on FO performance was investigated. Like the commercial CTA FO membrane, the resultant membranes showed relatively low water permeability compared to other recently developed TFC FO membranes, due to the denser structure of their skin layer (Fig. 11). The better FO performance of similar membranes (relatively thin, dense membrane embedded on a fabric support) compared to the performance of RO membranes is mainly attributed to their much lower thickness. The thickness of typical RO membranes is approximately 150–250 μm, while the thickness of commercial osmotic membrane is close to 50 μm.

CA membranes with top and bottom dense layers sandwiching a highly porous middle layer were recently prepared and investigated.[153,154,174,179] In this membrane the top-layer is considered to be the selective layer that determines the performance of the membrane. As discussed in earlier sections of this manuscript, the substructure plays an important role in ODMP membrane performance. The water flux in the FO configuration (active/dense layer facing the feed and porous support layer in contact

Table 5 Developed membranes and their properties and performance in FO and PRO processes

Name	Material skin/support (thickness, μm)	Testing configuration	Feed–draw test solution	$A \times 10^{-9}$ m s^{-1} kPa^{-1}	R (%)	$B \times 10^{-6}$ m s^{-1}	$K \times 10^{5}$ s m^{-1}	S (mm)	Performance (pressure driving force normalized) Flux $\times 10^{-6}$ m s^{-1} ($\times 10^{-10}$ m s^{-1} kPa)	Performance (pressure driving force normalized) W, W m^{-2} (mW m^{-2} kPa^{-1})	Note
Based on commercial membranes											
Asymmetric FO membrane											
HTI-CTA[114]	CTA	PRO	DI water–0.6 M NaCl	1.87	94	0.11	4.5	0.678	2.81 (15.79*)	2.73 (1.52)*	*At ΔP = 972 kPa
HTI-w fabric[148]	CTA (45)	PRO	0.01 M NaCl–0.5 M NaCl	0.90	81.1	0.040		1.00	1.82 (8.34)		
		FO	0.01 M NaCl–0.5 M NaCl						1.39 (6.37)		
HTI-nw fabric[148]	CTA (144)	PRO	0.01 M NaCl–0.5 M NaCl	1.30	92.4	0.027		1.38	2.28 (10.43)		
		FO	0.01 M NaCl–0.5 M NaCl						1.23 (5.63)		
Asymmetric NF/RO membranes											
CA-70[23]	CA	PRO	DI water–0.6 M NaCl	1.0	87	2	0.65		1.23 (9.81)	1.55 (1.24)	
CA-80[23]	CA	PRO	DI water–0.6 M NaCl	3.3	39	87	0.38		1.05 (8.40)	0.35 (1.06)	
BM-05/Berghof[23]	PA	PRO	DI water–0.6 M NaCl	0.4	90	0.23	19		0.31 (3.20)	0.31 (0.31)	
PBIL/Teijin[23]	PBIL	PRO	DI water–0.6 M NaCl	0.65	92	0.32	6.9		0.68 (5.91)	0.79 (0.67)	
TFC NF/RO membranes											
PA-300[23]	PA/PSf	PRO	DI water–0.6 M NaCl	1.1	99.3	0.17	57		0.23 (3.19)	0.17 (0.24)	
NS 101/North Star[23]	PA/PSf	PRO	DI water–0.6 M NaCl	1.2	94	0.44	290		0.03 (3.00)	0.003 (0.03)	
BM-1-C[23]	Unknown/PSf	PRO	DI water–0.6 M NaCl	0.80	89	0.61	40		0.17 (4.15)	0.07 (0.10)	
SW30-HR-nw fabric[120]	PA/PSf	FO	DI water–1.5 M NaCl	3.55	98.9	0.08		9.583	0.62 (0.81)		
SW30-HR-no fabric[120]	PA/PSf (35)	FO	DI water–1.5 M NaCl	4.06	98.3	0.11		2.155	2.02 (2.65)		
Lab-developed membranes											
Asymmetric membranes											
Double dense-layer CA[153]	CA (35)	FO	DI water–2.0 M NaCl	0.47	92.0	0.019		0.054	1.39 (1.29)		– Double dense-layer membrane: the denser layer is referred to as active layer
		PRO	DI water–2.0 M NaCl						1.58 (1.47)		
Single dense-layer CA[153]	CA (34)	FO	DI water–2.0 M NaCl	0.36	87.4	0.025		0.051	1.17 (1.08)		
		PRO	DI water–2.0 M NaCl						1.44 (1.34)		
Double dense-layer CA[154]	CA	FO	DI water–5.0 M $MgCl_2$	2.08	79	0.075			7.61 (1.62)		– AL refers to the thinner top-layer at the interface between casting polymer and substrate
		PRO							13.39 (2.86)		
CA13.9g-Lac6.3g[155, 156]	CA (70–80)	PRO	0.6 M NaCl–1.25 M $MgSO_4$	1.22	100	0			1.22 (12.2)		– CA was cast on nylon fabric
CA13.9g-Lac6.3g-50/60	CA (70–80)	PRO	0.6 M NaCl–1.25 M $MgSO_4$	0.53	99	0.005			0.53 (5.30)		
CA13.9g-ZnCl6.3g-50/60	CA (70–80)	PRO	0.6 M NaCl–1.25 M $MgSO_4$	1.36	99	0.014			1.36 (13.6)		– Rejection of $MgSO_4$
CA13.0g-ZnCl7.0g-50/60	CA (70–80)	PRO	0.6 M NaCl–1.25 M $MgSO_4$	1.89	99.9	0.002			1.89 (18.9)		
CA/CTA-ZnCl6.8g-50/60	CA-CTA (70–80)	PRO	0.6 M NaCl–1.25 M $MgSO_4$	1.52	98	0.031			1.52 (15.2)		
PAI 1#[157]	PAI (71)	FO	DI water–0.5 M $MgCl_2$	12.72	92.15	0.108			4.53 (12.18)		– PAI 2# membrane is an asymmetric membrane on PET woven fabric
		PRO	DI water–0.5 M $MgCl_2$						5.47 (14.72)		
PAI 2#[157]	PAI (55)	FO	DI water–0.5 M $MgCl_2$	21.00	87.45	0.301			5.33 (14.34)		
		PRO	DI water–0.5 M $MgCl_2$						6.64 (17.85)		
PAI 2#-S[157]	PAI (55)	FO	DI water–0.5 M $MgCl_2$	41.00	64.82	2.269			3.18 (8.56)		
		PRO	DI water–0.5 M $MgCl_2$						8.24 (22.15)		
SUB-90[134]	CA (118)	FO	DI water–1.0 M $MgCl_2$	2.694	74.10	0.053	6.84		1.25 (1.33)		– Hollow fiber membrane – Membranes was treated at different temperatures
		PRO	DI water–1.0 M $MgCl_2$						6.94 (7.41)		
SUB-50[134]	CA (94)	FO	DI water–1.0 M $MgCl_2$	2.50	86.37				2.25 (2.40)		
		PRO	DI water–1.0 M $MgCl_2$						8.06 (8.59)		

Table 5 (*continued*)

Name	Material skin/support (thickness, μm)	Testing configuration	Feed–draw test solution	$A \times 10^{-9}$ m s^{-1} kPa^{-1}	R (%)	$B \times 10^{-6}$ m s^{-1}	$K \times 10^{5}$ s m^{-1}	S (mm)	Performance (pressure driving force normalized) Flux $\times 10^{-6}$ m s^{-1} ($\times 10^{-10}$ m s^{-1} kPa)	Performance (pressure driving force normalized) W, W m^{-2} (mW m^{-2} kPa^{-1})	Note
A-FO[158]	PES	FO	DI water–0.5 M NaCl	2.6	78	0.081	1.37		1.39 (6.25)		– Hollow fiber membrane
		PRO	DI water–0.5 M NaCl						3.58 (16.13)		
B-FO[158]	PES	FO	DI water–0.5 M NaCl	2.22	91	0.056	0.56		3.89 (17.50)		
		PRO	DI water–0.5 M NaCl						8.94 (40.26)		
TFC membranes											
TFC-FO[120]	PA/PSf (100)	FO	DI water–1.5 M NaCl	3.18	97.4	0.13		0.492	5.04 (6.62)		
9PSf-100NMP[159]	PA/PSf (95)	FO	DI water–1.0 M NaCl	4.53	95.8	0.23		0.389	5.69 (11.7)		– Porous support with different pore structures (sponge- or finger-like)
9PSf-100DMF[159]	PA/PSf (75)	FO	DI water–1.0 M NaCl	5.28	98.6	0.09		0.312	6.94 (14.35)		
12PSF-100NMP[159]	PA/PSf (75)	FO	DI water–1.0 M NaCl	2.89	96.7	0.18		0.530	3.86 (7.98)		
12PSF-50DMF-50NMP[159]	PA/PSf (75)	FO	DI water–1.0 M NaCl	2.58	97.7	0.08		0.577	3.47 (7.17)		
12PSF-100DMF[159]	PA/PSf (75)	FO	DI water–1.0 M NaCl	4.86	98.5	0.09		0.502	4.89 (10.10)		
LP[22]	PA/PSf (40)	PRO	DI water–0.5 M NaCl	4.53	95	0.031		0.349	4.63 (37.04)	5.79 (4.44)	– PRO performance was calculated using model for river and sea water
MP (AL modification)[22]	PA/PSf (40)	PRO	DI water–0.5 M NaCl	12.08	88	0.211		0.340	7.37 (58.96)	9.21 (7.06)	
HP (AL modification)[22]	PA/PSf (40)	PRO	DI water–0.5 M NaCl	20.99	68	1.244		0.360	4.98 (39.84)	6.23 (4.78)	
TFC-1[148]	PA/PSf (76)	PRO	0.01 M NaCl–0.5 M NaCl	3.2	94.5	0.047		0.71	5.03 (23.06)		– Two porous supports with finger-like structures but different pore sizes and porosity
		FO	0.01 M NaCl–0.5 M NaCl						2.65 (12.14)		
TFC-2 (LiCl)[148]	PA/PSf (73)	PRO	0.01 M NaCl–0.5 M NaCl	5.0	93.4	0.094		0.67	5.69 (26.12)		
		FO	0.01 M NaCl–0.5 M NaCl						3.33 (15.29)		
TFC[160]	PA/PSf (70)	PRO	DI water–2.0 M NaCl	4.0	95.6	0.039		0.782	9.44 (8.75)		– TNC membranes cooperate NaY zeolite (40–150 nm) in PA selective layer
		FO	DI water–2.0 M NaCl						3.89 (3.60)		
TNC0.1[160]	PA-Zeolite/PSf (70)	PRO	DI water–2.0 M NaCl	7.15	77.1	0.437			13.54 (12.54)		
		FO	DI water–2.0 M NaCl						5.90 (5.47)		
PES/SPSf TFC[161]	PA/PES-SPSf (115)	PRO	DI water–2.0 M NaCl	2.14	93.5	0.031	1.86	0.238	13.19 (12.22)		
		FO							7.22 (6.99)		
50 sulfonated polymer[162]	PA/PESU-*co*-sPPSU (40–55)	PRO	DI water–2.0 M NaCl	2.03	91	0.069	2.14	0.324	9.17 (8.49)		
		FO							5.83 (5.4)		
NC-FO-50[163]	PA/PES fiber (50)	FO	DI water–0.5 M NaCl	4.72	97.0	0.35		0.080	10.50 (47.26)		– NC-FO used a support prepared by electrospinning
NC-FO-70[163]	PA/PES fiber (70)	FO	DI water–0.5 M NaCl	4.58	97.0	0.34		0.106	9.42 (42.39)		
PI-FO[163]	PA/PES (100)	FO	DI water–0.5 M NaCl	3.47	96.5	0.30		0.450	3.72 (16.75)		
CAP-II-TFC[164]	PA/CAP	PRO	DI water–2.0 M NaCl	3.94	90.5	0.037		0.695	9.72 (9.01)		
		FO							4.63 (4.29)		
3#LbL-PAN[165]	PAH-PSS/PAN (60)	PRO	DI water–1.0 M $MgCl_2$	28.4	64	0.96		0.5	8.81 (11.83)		– The PE top-layer was prepared *via* the LbL technique
		FO	DI water–1.0 M $MgCl_2$	20.2	80	0.30		0.5	7.97 (10.66)		
6#LbL-PAN[165]		PRO	DI water–1.0 M $MgCl_2$						6.97 (9.36)		
		FO	DI water–1.0 M $MgCl_2$						6.11 (8.20)		

Table 5 (*continued*)

Name	Material skin/support (thickness, μm)	Testing configuration	Feed–draw test solution	$A \times 10^{-9}$ m s^{-1} kPa^{-1}	R (%)	$B \times 10^{-6}$ m s^{-1}	$K \times 10^{5}$ s m^{-1}	S (mm)	Performance (pressure driving force normalized) Flux $\times 10^{-6}$ m s^{-1} ($\times 10^{-10}$ m s^{-1} kPa)	Performance (pressure driving force normalized) W, W m^{-2} (mW m^{-2} kPa^{-1})	Note
LbL3-PAN[166]	PAH-PSS/PAN (55)	PRO	DI water–1.0 M $MgCl_2$	27.22	91.2	0.57			23.89 (32.09)		– The xLBL-PAN membrane series contains a cross-linked skin layer – xLbL3-3-PAN contains double skin layer for a better antifouling property
		FO	DI water–1.0 M $MgCl_2$						12.22 (16.42)		
xLbL3-PAN[166]		PRO	DI water–1.0 M $MgCl_2$	19.17	94.2	0.25			23.33 (31.35)		
		FO	DI water–1.0 M $MgCl_2$						9.44 (12.69)		
xLbL3-3-PAN[167]		PRO	DI water–1.0 M $MgCl_2$	8.9	93.2	0.14			11.75 (15.87)		
		FO	DI water–1.0 M $MgCl_2$						8.33 (11.25)		
#A-FO[158]	PA/PES (215)	PRO	DI water–0.5 M NaCl	2.6	78	0.081	9.09	1.37	3.58 (16.13)		– Very hydrophilic hollow fiber membranes
		FO	DI water–0.5 M NaCl						1.39 (6.25)		
#B-FO[158]	PA/PES (180)	PRO	DI water–0.5 M NaCl	6.2	91	0.056	4.0	0.595	8.94 (40.27)		– RO-like skin layer with 300–600 nm PA film thickness
		FO	DI water–0.5 M NaCl						3.89 (17.51)		
#C-FO[131, 168]	PA/PES (205)	PRO	DI water–0.5 M NaCl	9.72	95	0.062	3.41	0.55	11.83 (54.27)		
		FO	DI water–0.5 M NaCl						5.28 (24.21)		
PRO-TFC[169]	PA/PES (200)	PRO	River water (10 mN NaCl–0.5 M NaCl	9.22	—	0.039		0.46	13.11 (83.46)	11.0 (13.0)	– PRO-TFC was test in PRO set-up with 8.4 bar pressure applied
TFC-$PES_{water/NMP}$[170]	PA/PES (100)	PRO	DI water–2.0 M NaCl	4.56	83	0.078	1.65	0.252	15.86 (14.70)		– Hollow fiber membrane with macrovoid-free structure
		FO							8.92 (8.26)		
PAI#2-RO[171]	PA/PAI (175)	PRO	DI water–2.0 M NaCl	8.44	99.5	0.059			12.86 (11.92)		– DS#2-RO/NF contains double skin layers
DS#2-RO/NF[171]	PA/PAI (175)/ PAH-PSS	PRO		5.69	85.3	0.063			11.47 (10.63)		– RO-like skin was prepared *via* interfacial polymerization
		FO							4.72 (4.37)		– NF-like skin was prepared *via* LbL

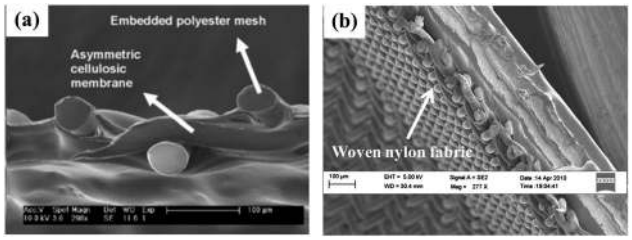

Fig. 11 SEM cross-sectional images of (a) commercial CTA HTI membrane and (b) the laboratory-made CA membrane ((a) is adapted from ref. 111 and (b) was adapted from ref. 155. Copyright 2011 with permission from Elsevier).

with the draw solution) is normally lower than that of membranes in the PRO mode (draw solution in contact with the feed) (see Table 5 for comparison), due to a more severe dilutive ICP in the porous support layer.[33,108,180] In the dual-layer membrane, it was found that a higher flux was obtained when the bottom layer faced the draw solution, and it was believed that the bottom layer might form a denser, more selective layer than the top selective layer.

Zhang *et al.* further studied double-sided dense CA membranes (Fig. 12).[153] The hydrophilicity of the casting substrate during the phase inversion process was reported to affect the structure of the bottom layer.[153,181] In the case of CA, the good hydrophilic interactions of the CA solution and the glass substrate resulted in dense layers. On the other hand, with a hydrophobic Teflon substrate, a porous structure was obtained at the bottom, while the top skin layer remained the same. This concept was further proved by applying different types of CA on different supports.[174] A typical membrane structure consisting of two dense membrane surfaces, two more porous sub-layers, and a very porous middle layer is shown in Fig. 12.

The salt rejection and permeability results also suggested that it was better to use the bottom layer as the selective layer than the top layer. Although the formation of the second dense layer led to additional water resistance and thus a lower flux in FO testing mode, it showed a potential in FO-membrane bioreactors (MBR).[153,154] The performances of membranes

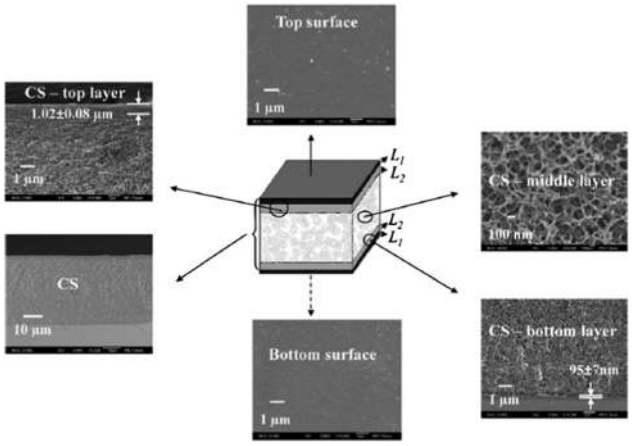

Fig. 12 Schematic diagram of three-sub-layer structured CA membranes. Reprinted with permission from ref. 153. Copyright 2011, Elsevier.

having single-dense-layer and double-dense-layer were compared in an FO-MBR configuration (submerged membranes) with aluminum oxide colloidal particles of approximately 200 nm diameter as model foulants. The double-dense-layer membrane was less susceptible to fouling compared to the single-dense-layer membrane. Its flux performance after washing and cleaning remained similar to the fluxes of the fresh membranes. However, the claim for better fouling resistance of the double-dense-layer membrane required additional support. If the membranes are exposed to smaller foulant molecules, clogging of the inner porous structure might be unavoidable. The fouled membrane will be even more difficult to clean with the presence of the second skin layer.

8.2.2 Thin-film-composite membranes. The formation of thin-film-composite TFC membranes offers the possibility to optimize support and selective layers separately. Such membranes are generally viewed to be a better fit for ODMPs where the structural parameter plays a significant role. Various morphologies of selective layers and their TFC membrane supports designed for ODMPs are shown in Fig. 13. Optimization is required to combine good salt retention of the selective layer with low ICP in the porous support layer to enable high water flux. In this section several strategies recently applied for the development of support and skin layers to obtain optimal performance are presented and discussed.

(1) Support layers. The physicochemical properties of the support layer are important to subsequently form a good selective skin layer at the substrate surface.[161] As discussed in earlier sections of this manuscript, the support layer of ODMP membranes should be thin, highly porous, and possess a low tortuosity to enable high flux and diffusion of draw solution solutes into the pores and back side of the active/dense layer. Recently, a number of membranes specially designed for ODMPs have been introduced.[22,120,148,159,182,183] Polysulfone (PSf) is one of the most widely used support materials for traditional RO-TFCs and has consequently been widely studied for TFC ODMP membranes.[22,120,159,184]

Tiraferri *et al.* investigated the influence of the structural parameter (S) of PSf membranes prepared *via* phase inversion.[159] The support morphology was optimized to accomplish a structure that allows the later formation of a selective skin-layer. Although substrates with more open pores facilitated water flow, wide pore openings resulted in uneven coatings of the selective layer and high salt leakages. To form a good skin layer by interfacial polymerization, a sponge-like structure of the top layer is claimed to be preferred, while membranes with open finger-like pores or a highly porous bottom skin enhance the flux and the transport of leaked salts.[159] Yip *et al.* successfully combined both requirements and prepared TFC-PSf supports with a sponge-like structure on top of a finger-like structure.[120] The structural parameter of the prepared membranes was lower than 500 microns and good performance was achieved, including a water flux higher than 5 μm s^{-1} (18 L m^{-2} h^{-1}) and NaCl rejections greater than 97%. Moreover, the resultant membranes were not degraded after being exposed to an ammonium bicarbonate (NH_3HCO_3) draw solution at elevated pH.

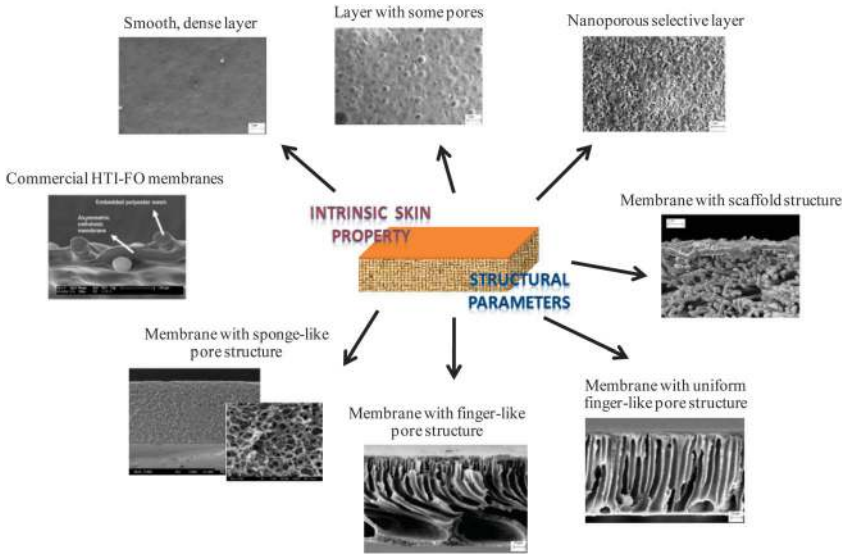

Fig. 13 Schematic of TFC membranes with various substrate and skin layer properties compared to the commercial FO membranes (asymmetric membrane from HTI). SEM micrographs were adapted from ref. 111, 148, 153 and 163 with permissions from Elsevier and Wiley.

This made the prepared membranes superior to CA membranes, which are chemically unstable at high and low pHs.[120]

It is well accepted that increasing the membrane hydrophilicity is another effective approach to improve water flux, as it promotes wetting of all available pores.[183] Several additives such as polyethylene glycol (PEG) and polyvinylpyrrolidone (PVP) have been used to improve the hydrophilicity and porosity of the PSf substrates, but lower fluxes were observed in the case of TFC membranes made of these substrates.[185] This is mainly due to the formation of a dense polyamide (PA) layer inside the pores during the interfacial polymerization step, which later obstructs the water flux. Moreover, these additives gradually leached out from the membrane during operation, which could cause membrane instability. Wang *et al.* recently developed substrates for TFC-FO membranes from blends of polyethersulfone (PES) and sulfonated PSf (sPSf) to increase the hydrophilicity of the PES.[161]

In fact, the ideal membrane support-layer morphology for ODMP membranes is still under debate. The porous support layer with straight finger-like pore structure is thought to have more advantages due to its low pore tortuosity that could favour the transport of both water and salt.[159] Some investigations, on the other hand, suggested that a porous support layer with a sponge-like macrovoid-free support layer is essential for the formation of sufficiently selective skin and for a better mechanical support.[162,164] Li *et al.* and Widjojo *et al.* extensively investigated the effect of membrane structures on their performance.[162,164] They found that it is not always required for membranes to have finger-like structure in order to obtain a low structural parameter that suppresses ICP and enhances water flux. Specifically, once the membrane comprises high hydrophilic characteristics, the structural parameter can also be remarkably reduced, though the substrate exhibits macrovoid-free structure.[162]

Electro-spun PES fibers were prepared and used as the support layer for ODMP TFC membranes.[163] Substrates with high porosity, low tortuosity, and very low structural parameter (80–100 microns) were obtained (Fig. 14).[163] Superior performance was noticed with water flux of up to 10.5 μm s^{-1} (38 L m^{-2} h^{-1}) (tested with 0.5 mol L^{-1} NaCl draw solution), even when the membrane was configured in FO mode (dense layer in contact with feed). In general, the water flux of most membranes reported in the literature was limited to 5–7 μm s^{-1} when tested in FO configuration (Table 5). Compared to TFC membranes with a PES support prepared *via* phase inversion, the TFC membranes with nanofiber supports (*via* electro-spinning) exhibited similar NaCl rejections and slightly higher permeability. The higher flux through the nanofiber membranes was attributed to their smaller structural parameter. Recently, focus has shifted to electro-spun nanofiber membranes.[186,187] Although high performance was reported, the mechanical stability of the selective film deposited directly on the electro-spun nanofiber support is still uncertain.[186,187] Hoover *et al.* suggested the use of the electro-spun nanofiber as the backing support to enhance the mechanical properties of the ODMP TFC membrane.[187] Though the water permeability of the membranes slightly decreased, membrane mechanical stability increased, making the membrane more suitable to sustain handling and fluid shear forces under the real operating conditions of ODMPs.[187]

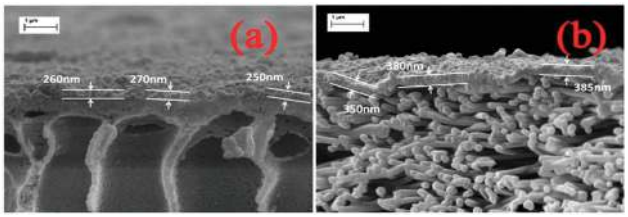

Fig. 14 Cross-sectional SEM images of TFC membranes from (a) PES support prepared by phase inversion and (b) PES nanofibers prepared by electrospinning. Reprinted with permission from ref. 163. Copyright 2011, Wiley.

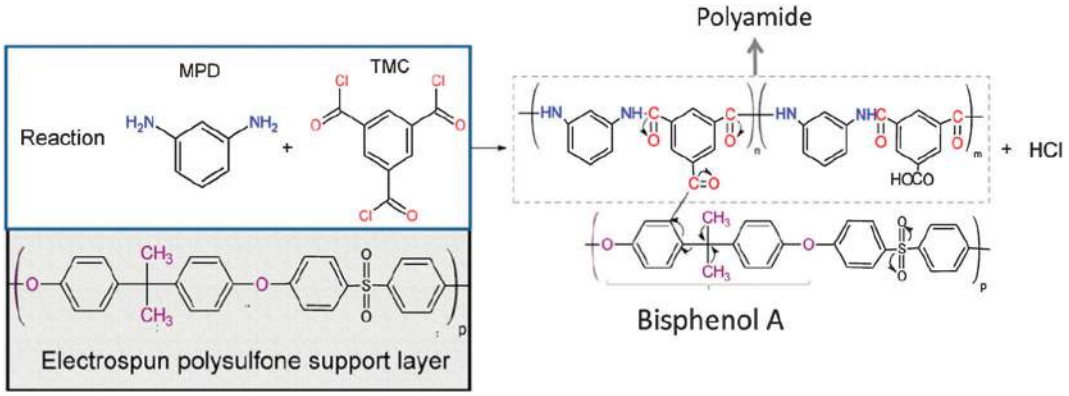

Fig. 15 Proposed cross-linking reaction between PA and the biphenol A group of PSf. Reprinted with permission from ref. 186. Copyright 2011, Elsevier.

The result from these works, in fact, has boosted research attention to explore new types of membrane structures that might be promising for the engineered osmosis field. In addition, there is a high potential to further improve the nanofiber support *via* electro-spinning with additional desirable properties such as tuneable hydrophilicity and bactericidal properties.[188–192]

(2) Selective skin-layers

Interfacial polymerization. Interfacial polymerization (IFP) is a widely used technique to deposit a thin selective layer on a porous support layer. In the IFP process, polymerization reaction takes place at the interface between two immiscible solvents containing very reactive monomers. The support material plays a crucial role in the final quality of the deposited film. During the polymerization, the support serves as a reservoir for one of the monomers and defines the interface where the reaction occurs. Two types of monomers are commonly used in IFP. These include aliphatic or aromatic diamines such as piperazine (PIP), *m*-phenylenediamine (MPD), or *p*-phenylenediamine (PPDA); or acid chlorides such as trimesoyl chloride (TMC), isophthaloyl chloride (IPC), 5-chloroformyloxyisophthaloyl chloride (CFIC), or 5-isocyanatoisopthaloyl chloride (ICIC).[193] Among these monomers, the PA film from IFP of MPD and TMC is most studied. PA based membranes possess superior properties of a high flux, good salt and organic rejection, and stability under a wide range of operating conditions. Therefore, the PA membranes are widely used in many separation processes and dominate the market for RO desalination membranes.[194] In fact, most commercial TFC RO membranes and most ODMP TFC membranes under current developments are PA-based membranes. To date, for ODMP membranes, most efforts were directed towards membrane structural modification, but less to the optimization of the skin IFP layer.[194]

To a large extent, IFP optimization is still aiming at improving membrane performance in pressure-driven membrane processes. With different chemistry and structure of the support layers for pressure-driven membrane processes or for ODMPs, optimization conditions may not be similarly applicable. The key parameters for IFP include morphology and properties of the support, monomer selection and concentration, additives, and reaction conditions.[193,195–201]

Support properties. The selected support materials limit the choice of monomers depending on the compatibility and chemical resistance of the support and monomers.[185,202,203] The adhesion of the PA film to a PSf support was found to be better than to a PES support.[186] The slight difference in hydrophilicity between the polymers could not explain the difference in adhesion properties. Cross-linking between the PA and the biphenol A groups of PSf was suggested as another reason for difference in adhesion (Fig. 15).

Monomers. The MPD–TMC monomer pair has been used most often for the formation of selective layers of TFC ODMP membranes.[22,120,131,148,159–164,168,169,186] The monomer system selection for PA film formation is critical to promote high salt rejection and water flux in pressure driven membranes. Wei *et al.* recently investigated the formation of PA selective layers by IFP on top of PSf support layers, focusing on the effects of monomer concentration on the quality of the formed skin layers.[194] The concentration of MPD and TMC had a significant impact on thin PA film formation, where a denser structure resulted from increasing MPD concentrations. On the other hand, the increase in TMC concentration resulted in excess unreacted acyl chloride groups and consequently a decline in the degree of cross-linking, but good water permeability. For FO applications, it is well established that the performance of membranes is also dependent on the ratio of water flux to salt reverse flux (J_w/J_s). The prepared membranes were tested at two different draw solution concentrations. At high concentration, the membrane selectivity became dominant because of the J_s-induced ICP (tendency of enhanced reverse salt flux at high concentration).

It is important for membranes to have a good selective surface when operating with high draw solution concentrations to prevent reverse diffusion of solutes and suppress ICP. Increasing MPD concentration resulted in good salt retention and increased water flux (PRO configuration). The opposite trend was observed in the case of increasing TMC concentration.

Additives. Some additives have been reported to promote the formation of selective films.[195] The introduction of additives can also offer other benefits during synthesis with IFP, including enhancing the diffusion of the monomers to the interface,

improving the wettability of the top surface of the support, and acting as a buffer agent that helps capturing byproducts and controlling reaction pH.[199]

In addition to improving film formation during the IFP process, some inorganic additives such as TiO_2, silica, and zeolite nanoparticles were added to the monomer solutions to modify the transport properties and fouling resistance of the new membranes.[160,182,201,203–207] The addition of these nanoparticles was also expected to improve hydrophilic properties of the membranes. Consequently, not only membrane permeability was enhanced, but also its fouling resistance properties. For example, Ma *et al.* incorporated a small amount of NaY zeolite nanoparticles (40–150 nm) into the top PA skin film.[160] Water permeability of the modified PA selective skin was enhanced up to 80% and the water flux showed 50% improvement.

Layer-by-layer dip-coating. In addition to the widely used IFP technique, various coating techniques such as photografting, layer-by-layer dip-coating, and plasma-initiated polymerization have been applied for forming ultrathin layers on membranes.[165–167,171,208–211] *Via* the polyelectrolyte *Layer-by-Layer* (LbL) method, poly(allylamine hydrochloride) (PAH) and poly(sodium 4-styrene-sulfonate) (PSS) were deposited on a PAN support to form TFC ODMP membranes.[165–167]

Via such self-assembly of charged macromolecules, an ultrathin selective skin with controlled thickness in the nanometer range can be prepared on a porous support.[212,213] The structure and properties of the films can be simply designed by a proper choice of the chemical construction parameters.[213] However, the balance of charge density is critical and much care is required when fabricating films *via* this technique.

The LbL membranes exhibited good FO performance with high fluxes of 4.17 $\mu m\ s^{-1}$ (15 $L\ m^{-2}\ h^{-1}$) using a 0.1 M $MgCl_2$ draw solution. However, the prepared LbL membranes experienced a decline in salt rejection when the active layer was facing high ionic strength solutions.[165] Later, Qiu *et al.* tried to eliminate this problem by introducing crosslinking in the membrane.[166] The reduction of salt rejection with high electrolyte concentrations was successfully diminished, but the water flux decreased due to the denser skin layer. Although the results show high fluxes, one should keep in mind that this membrane was tested with a $MgCl_2$ electrolyte solution in which the cation hydrate size is much larger than in NaCl.[14,122]

(3) Membrane post-treatment and modifications. A post-treatment step has proved to play an essential role in improving the separation performance of newly formed ODMP membranes.[214] In addition, for the fabrication of TFC membranes, the post-treatment of the membrane substrate prior to the deposition of the selective layer can strongly affect the final quality of the film. The post-treatment conditions are specific for each type of membrane. It is crucial to understand the rationale behind different treatment conditions and it requires the right practice, because it can either improve or degrade the membrane properties. In addition, some post-treatment techniques are performed to preserve the pore structure of the membranes.[134,158,215]

Increasing membrane selectivity. Thermal treatment is one of the most common post-synthesis treatment techniques. It is used mainly for reducing the pore size of membranes and thus improving selectivity. For ODMPs, such good retention clearly helps preventing reverse salt diffusion and ICP effects inside the membrane porous support layer. For example, CA membranes showed 80% increase in salt rejection after heat treatment at 90 °C for 15 min.[153] However, such thermal treatment mostly coincides with a lower permeability due to the shrinkage of the pores.

Additionally, thermal treatment of PA films was reported as a crucial curing step for the IFP reaction. The curing step helped removing the residual solvent from the film and promoted further crosslinking.[196,199,216,217] PA films from MPD and TMC or CFIC exhibited better selectivity after curing at 45–90 °C for 3–20 min.[196,216,217] In fact, the permeability of the membrane also increased; however, extreme curing conditions at higher temperatures and longer curing periods resulted in the loss of both permeability and selectivity.[196,216,217]

Increasing permeability. Common post-treatment procedures to improve membrane permeability are (1) tuning hydrophilicity and wetting properties of the membranes and (2) widening the pore size or increasing the free volume for dense materials in the selective skin and loosening the membrane structure. The result of simultaneous loss of selectivity can often not be avoided for the second approach. Yu *et al.* investigated the influence of different post-treatment conditions on water flux of TFC membranes, and results are summarized in Table 6.[217]

Exposing TFC membranes to a chlorine solution followed by an alkaline solution was used to loosen the film structure and thus improve water flux through the membranes.[22] The flux through the TFC membrane was increased several times, depending on the post-treatment conditions, which consisted of soaking the membrane at different concentrations of chlorine and alkaline solution for different lengths of time. However, this treatment method generally reduced the rejection ability of the selective layers. The treatment steps thus have to be carefully controlled to not destroy the selective properties of the membranes.

8.2.3 Trade-off in ODMP membrane performance. Recently, a permeability–selectivity trade-off was established for polymeric desalination membranes, similar to that in gas

Table 6 Water flux and salt rejection of TFC membranes prepared from MPDA-CFIC followed by different post-treatment conditions[217]

Post-treatment	Water flux (10^{-6} m s^{-1})	Salt rejection (%)
As prepared membrane	9.6	99.4
Soaked in 30 wt% methanol at 40 °C for 10 h	11.1	99.2
Soaked in 20 wt% TEA and 1.0 wt% NaOH at 40 °C for 2 h	11.0	99.4
Soaked in 200 ppm hypochlorite (pH 12) at room temperature for 2 h	11.0	99.4
Soaked in 60 °C pure water for 1 h, followed by 200 ppm hypochlorite (pH 12) at room temperature for 2 h	11.4	99.4

Testing conditions: 3.5 wt% NaCl; 5.5 MPa.

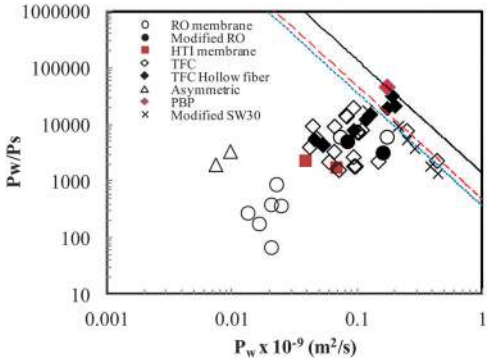

Fig. 16 Correlation between water/NaCl permeability–selectivity (P_w/P_s) and water permeability (P_w) of ODMP membrane (data from Table 5). The solid black line represents the proposed upper bound relationship of the desalination membranes adapted from Geise *et al.* (λ = 1.4 × 10^{-15} m^4 s^{-2} and β = 2).[218] The blue dotted line is the trade-off for the modified polyamide active layer for ODMPs currently proposed by Yip and Elimelech (λ = 0.37 × 10^{-15} m^4 s^{-2} and β = 2).[127] The dashed red line indicates the trade-off for flat sheet membranes proposed by this review for flat sheet osmotic membranes currently being developed.

separation.[218,219] Using a similar approach, the water permeability (P_w) and the water/salt (specifically, NaCl) permeability selectivity P_w/P_s can be calculated by the following empirical equation:

$$\frac{P_w}{P_s} = \frac{\lambda}{(P_w)^{\beta}} \quad (30)$$

where λ and β are the empirical fitting parameters. The water and salt permeability, P_w and P_s, are related directly to the intrinsic properties, A and B, of the active layer as shown in eqn (31) and (32):

$$P_w = AL\frac{\rho R_g T}{M_w} \quad (31)$$

$$P_s = BL \quad (32)$$

where L is the thickness of the active layer, M_w the molar mass of water, R_g the gas constant, T the absolute temperature and ρ is the density of water. Using literature data (*e.g.*, data in Table 5), an upper boundary trade-off of the membranes in ODMPs was observed (Fig. 16).

It is worth noting that the empirical parameters λ and β of membranes in desalination are hypothesized to possess similar fundamental physical meanings as in gas separation. However, there are no sufficient data to suggest such a physical meaning in desalination yet.[218] To perform the fitting, the value β = 2 was adopted from previous studies.[127,219] Due to the lack of accurate reports of selective skin thickness, it is assumed to be 150 nm. This is considered to be a reasonable value because most PA thin films were reported to form a layer with 40–300 nm thickness.[127] From Fig. 16 it can be seen that TFC ODMP membranes exhibit permeability–selectivity trade-off with an upper bond layer of λ = 0.48 × 10^{-15} m^4 s^{-2}, which is still lower than commercial pressure-driven membranes for desalination. However, some recently developed TFC hollow fiber membranes achieved permeability–selectivity behavior close to the upper bound of commercial RO membranes.

Membranes achieving high water permeability are always accompanied by high salt permeability. As discussed earlier, this is vital especially in ODMPs, because high reverse salt fluxes have negative consequences such as exacerbated ICP and chemical demands. In fact, the reverse salt flux is also dominated largely by the properties and structural parameter (S) of the support layer, which determines how well the leaking salts can be transported to the bulk solution.

Fig. 17 illustrates a survey of water fluxes from currently developed ODMP membranes plotted against three main key intrinsic membrane properties. The structural parameter showed a clear influence on membrane performance, which in fact agrees well with the performance predictions from early theoretical and modeling studies.[147] In addition, the optimization of membrane skin properties (A/B) was found to be closely

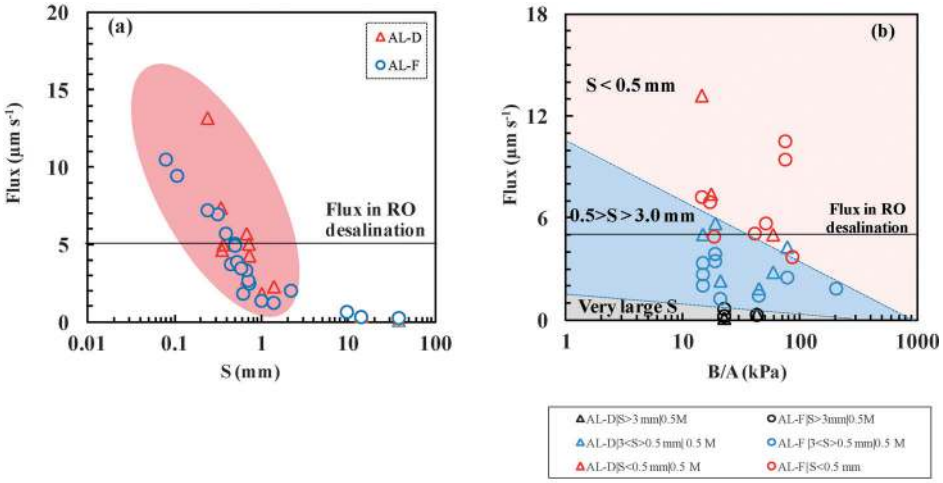

Fig. 17 Flux of currently developed membranes as a function of the (a) S parameter and (b) B/A ratio. The developed membranes were oriented in FO (circle symbol) and PRO (triangle symbol) configuration and tested with 0.5–2 M NaCl draw solutions under FO process conditions. (The data in the plots are from Table 5.)

related to the structural parameter. Typically, membranes with low structural parameter are able to bear higher B values. Low structural parameter membranes showed good water flux and good mass transport from the salt to the bulk solution. In fact, the salt leakage (inducing ICP) seemed less important for low structural parameter membranes. It is the A value that plays the most important role. On the other hand, for membranes with a high S-value, an even small salt leakage can already cause severe ICP. These results provide a useful guideline to further optimize the skin properties for ODMP membranes based on different support structures.

9. Summary and future perspective

This review provides a summary of current progress in ODMPs, with a main emphasis on transport modelling and material development. The profound understanding of transport behaviour is of importance for future process design, as well as for further membrane development and optimization. Reducing ICP, a phenomenon unique to ODMPs that can dramatically reduce the osmotic driving force and consequently reduce water fluxes, is currently the main research area because it is considered the biggest barrier for breakthrough in engineered osmosis applications. Several models have been developed over the last two decades to explain the ICP and related transport phenomena in ODMP membranes. Though the ODMPs seem simple at first glance, their optimization is not simple because flux equations and moduli of ICP and ECP are in a complex relationship with each other. In addition, process operating conditions and properties of working solutions, *i.e.* flow rate, temperature, concentration, viscosity, and diffusivity of feed and draw solution, also play a role in ODMP performance. Among those parameters, the physicochemical properties of solute and concentration of draw solutions have been studied most intensively, mainly because they were found to have a significant impact on CP and membrane performance. ECP and ICP can be reduced to some extent by adjusting process and membrane parameters. However, the most effective approach is the tailoring of properties and structures of the membrane – the key element in ODMPs. Like other membrane processes, ODMP membranes are controlled by water/salt permeability selectivity trade-off. In addition, in ODMPs water flux itself is self-limiting. Recent fundamental studies reveal that water flux in ODMPs is involved in other challenges. In addition to forming a complex relationship with ECP, ICP, and reverse salt flux, water flux also has a strong influence on fouling.

PRO is often viewed as a special application branch for FO membranes for which limited experimental data exist. However, membranes that work well in one particular system may not be able to offer the same performance once applied under different operating conditions of related processes (*e.g.*, PRO). Therefore, it is still unclear if newly developed FO membranes can work well for PRO, and thus more membrane development and PRO investigations are needed.

Around the world we see high demand for new renewable energy resources, and there is of course an urgent need for more fresh water. And we also increasingly see the close interplay between water and energy. Desalination became one of the best approaches to produce fresh water from abundant seawater. Current state-of-the art RO desalination produces high quality water at a cost of 2–4 USD per 1000 gallons with an energy consumption of 10–60 kJ per kg of fresh water.[220] Depending to a certain extent on plant size, these techno-economical properties of seawater RO pose a high barrier for other technologies to penetrate the market. However, energy scarcity is currently driving RO to further reduce its energy consumption. FO is thus gaining increasing attention as an alternative process, requiring less energy and less pre-treatment. The big barrier for FO desalination is the separation and re-concentration of the draw solution. On the other hand, used as a pre-treatment unit in RO desalination, FO could save as much as 30% of the desalination cost and substantial energy consumption.[11,19,221] With the worsening global water situation, societies will be forced to recover water from marginal resources such as gray water or sewage and ODMPs might gain even more attention. Further investigations of ODMP applications with various feed and draw solutions are thus required to prove novel concepts that were recently proposed (*e.g.*, hybrid FO–RO for water augmentation or the FO for fertigation). By combining PRO with RO or FO/RO, cogeneration of power and clean water may be realized, and energy consumption of RO desalination could be further reduced.

The growing awareness of water and energy scarcity has pushed tremendous efforts to search for a sustainable solution. Today, research and development of ODMPs as emerging technologies is taking place in many countries around the world. Considering promising energy-saving processes for water purification and clean renewable energy technologies, ODMPs are gaining global attention and receiving more research and development funding from industry and governments. Examples of these funded projects are the ''Mega-ton-water project'' in Japan, seaHERO in Korea, and the OMEGA project in the USA (funded by NASA Ames Research Centre).[221,222] More pilot and demonstration plants utilizing osmotic effects have been established over recent years,[222] and more ODMP membranes are being developed. HTI has recently developed a new FO-TFC membrane, possessing a better performance than the first-generation HTI-CTA membrane.[223] In addition, Porifera has recently announced that they also successfully developed novel TFC FO membranes ready for commercial production.[208,222]

Though the progress in the development of ODMPs has been rapidly growing, there are still ample research needs in these technologies. A better understanding of the transport behaviour and fouling mechanism in osmotic processes, novel ideas in the development of ODMP membranes, the search for suitable draw solutions and their recovery processes, advanced systems and module designs, and the creativity to find new applications are greatly needed. Statkraft has predicted that if a full scale osmotic power plant of 25 MW is constructed, approximately 5 million m^2 of ODMP membranes will be required.[69] Furthermore, if 500 000 m^3 d^{-1} FO capacity is

installed over the next five years, it will require approximately 1.9 million m^2 of ODMP membranes (based on 3.75×10^{-6} m s^{-1} (13.5 L m^{-2} hr^{-1}) water flux).[6] This not only creates a new interesting market for ODMP membranes, but also increases potential markets for the polymer and membrane industries. The potential for ODMPs is enormous, but to make it feasible and sustainable, several technological developments, as well as large-scale investigations, are obviously still required. There is no doubt that ODMPs will play an increasing role in society as truly green and sustainable technologies, offering a significant contribution to the global water and energy supply.

Abbreviations

AA	Acetic acid
PRO mode	Membrane orientation where active layer faces draw solution
FO mode	Membrane orientation where active layer faces feed solution
BC	Benzoyl chloride
CA	Cellulose acetate
CAP	Cellulose acetate propionate
CDA	Cellulose diacetate
CECP	Concentrative external concentration polarization
CFIC	Chloroformyloxyisophthaloyl chloride
CICP	Concentrative internal concentration polarization
CP	Concentration polarization
CTA	Cellulose triacetate
CTAB	Cetyltrimethylammonium bromide
DECP	Dilutive external concentration polarization
DICP	Dilutive internal concentration polarization
ECP	External concentration polarization
EGMG	Ethylene glycol methyl ether
FO	Forward osmosis
ICIC	5-isocyanatoisopthaloyl chloride
ICP	Internal concentration polarization
IPC	Isophthaloyl chloride
NF	Nanofiltration
PA	Polyamide
PAI	Polyamide-imide
PAN	Polyacrylonitrile
PAS	Positron annihilation spectroscopy
PC	Phthloyl chloride
PDA	Phenylenediamine
PEG	Polyethylene Glycol
PEI	Polyethyleneimine
PES	Polyether sulfone
PI	Polyimide
PIP	Piparazine
PPDA	*p*-Phenylenediamine
PRO	Pressure retarded osmosis
PSf	Polysulfone
PS	Polystyrene
PSS	Poly(sodium 4-styrene-sulfonate)
PVDF	Thickness (m)
PVP	Polyvinylpyrolidone
RO	Reverse osmosis
SDS	Sodium dodecyl sulfate
sPEEK	Sulfonated poly(ether ether ketone)
sPSf	Sulfonated polyethersulfone
TEA	Triethylamide
TMC	Trimesoyl chloride
TPC	Terephthaloyl chloride
UF	Ultrafiltration
W	Power production (W m^{-2})

Nomenclature

A	Water permeability (m s^{-1} Pa^{-1})
B	Salt permeability coefficient (m s^{-1})
$C_{F,b}$, $C_{D,b}$	Salt concentration of the bulk feed and draw solution
$C_{F,i}$, $C_{D,i}$	Concentration of feed and draw solution near membrane surface inside porous supports
$C_{F,m}$, $C_{D,m}$	Concentration of feed and draw solution near membrane surface
C_p, C_f	Salt concentration in permeate and feed solutions
d_h	Hydraulic diameter (m)
D	Diffusion coefficient of solute (m^2 s^{-1})
D_o	The diffusion coefficient at an infinite dilution (m^2 s^{-1})
D_e	Effective diffusion coefficient (m^2 s^{-1})
J_w	Water flux (m s^{-1})
J_s	Salt flux (m s^{-1})
k	Mass transfer coefficient (m s^{-1})
k_c	The mean mass transfer coefficient (m s^{-1})
K	Solute resistivity (s m^{-1})
L	Length of the flow channel (m)
M	Molality
ΔP	Pressure difference (kPa)
R	Salt rejection
Re	Reynolds number
S	Structural parameter (m)
Sc	Schmidt number
Sh	Sherwood number
t	Thickness (m)
V_w	Partial molar volume of water (m^3 mol^{-1})
W	Power (W m^{-2})

Greek symbols

π	Osmosis pressure (Pa)
$\pi_{F,b}$, $\pi_{D,b}$	Osmotic pressure of the bulk feed and draw solution (Pa)
$\pi_{F,m}$, $\pi_{D,m}$	Osmotic pressure of feed and draw solution near membrane surface (Pa)
$\pi_{F,i}$, $\pi_{D,i}$	Osmotic pressure of feed and draw solution near membrane surface inside porous supports (Pa)
$\Delta\pi$, $\Delta\pi_{eff}$	Osmotic pressure difference and effective osmotic pressure difference (Pa)
ρ_w	Molar density of water (mol L^{-1})
ε	Porosity
σ	Reflection coefficient

η_w, η_s	Viscosity of water and solution (kg $m^{-1}s^{-1}$)
τ	Tortuosity (m)
γ	Activity coefficient

Acknowledgements

Chalida Klaysom and Ivo F. J. Vankelecom are grateful for the financial support from the OT (11/061) funding from KU Leuven, the I.A.P – P.A.I. grant (IAP 6/27 & IAP 7/05) from the Belgian Federal Government, and the long term Methusalem (CASAS) funding by the Flemish Government.

Notes and references

1 M. Elimelech and R. McGinnis, *Membr. Technol.*, 2009, **4**, 10–11.
2 Q. Schiermeier, *Nature*, 2008, **452**, 260–261.
3 M. Elimelech, *Science*, 2011, **333**, 712–717.
4 R. L. McGinnis and M. Elimelech, *Environ. Sci. Technol.*, 2008, **42**, 8625–8629.
5 S. Patel, *Osmotic Power Makes Headway, Power*, 2011, **155**, 13–14.
6 A new spin on forward osmosis, Houston, 2012.
7 R. J. Aaberg, *Refocus*, 2003, **4**, 48–50.
8 A. Achilli and A. E. Childress, *Desalination*, 2010, **261**, 205–211.
9 T. Y. Cath, A. E. Childress and M. Elimelech, *J. Membr. Sci.*, 2006, **281**, 70–87.
10 S. Zhao, L. Zou, C. Y. Tang and D. Mulcahy, *J. Membr. Sci.*, 2012, **396**, 1–21.
11 T. Y. Cath, N. T. Hancock, C. D. Lundin, C. Hoppe-Jones and J. E. Drewes, *J. Membr. Sci.*, 2010, **362**, 417–426.
12 L. Liu, M. Wang, D. Wang and C. Gao, *Recent Pat. Chem. Eng.*, 2009, **2**, 76–82.
13 Z. Y. Liu, H. W. Bai, J. Lee and D. D. Sun, *Energy Environ. Sci.*, 2011, **4**, 2582–2585.
14 A. Achilli, T. Y. Cath and A. E. Childress, *J. Membr. Sci.*, 2010, **364**, 233–241.
15 R. E. Pattle, *Nature*, 1954, **174**, 660.
16 L. A. Hoover, W. A. Phillip, A. Tiraferri, N. Y. Yip and M. Elimelech, *Environ. Sci. Technol.*, 2011, **45**, 9824–9830.
17 L. Chekli, S. Phuntsho, H. K. Shon, S. Vigneswaran, J. Kandasamy and A. Chanan, *Desalin. Water Treat.*, 2012, **43**, 167–184.
18 S. Zhao, L. Zou, C. Y. Tang and D. Mulcahy, *J. Membr. Sci.*, 2012, **396**, 1–21.
19 N. T. Hancock, N. D. Black and T. Y. Cath, *Water Res.*, 2012, **46**, 1145–1154.
20 J. R. McCutcheon and M. Elimelech, *AIChE J.*, 2007, **53**, 1736–1744.
21 S. Loeb, L. Titelman, E. Korngold and J. Freiman, *J. Membr. Sci.*, 1997, **129**, 243–249.
22 N. Y. Yip, A. Tiraferri, W. A. Phillip, J. D. Schiffman, L. A. Hoover, Y. C. Kim and M. Elimelech, *Environ. Sci. Technol.*, 2011, **45**, 4360–4369.
23 K. L. Lee, R. W. Baker and H. K. Lonsdale, *J. Membr. Sci.*, 1981, **8**, 141–171.
24 S. Loeb, *J. Membr. Sci.*, 1976, **1**, 49–63.
25 G. D. Mehta and S. Loeb, *J. Membr. Sci.*, 1978, **4**, 261–265.
26 A. Seppälä and M. J. Lampinen, *J. Membr. Sci.*, 1999, **161**, 115–138.
27 S. Loeb, T. Honda and M. Reali, *J. Membr. Sci.*, 1990, **51**, 323–335.
28 S. Loeb and G. D. Mehta, *J. Membr. Sci.*, 1978, **4**, 351–362.
29 A. Seppala and M. J. Lampinen, *J. Membr. Sci.*, 1999, **161**, 115–138.
30 F. Vigo and C. Uliana, *Desalination*, 1986, **60**, 54–57.
31 M. Reali, G. Dassie and G. Jonsson, *J. Membr. Sci.*, 1990, **48**, 181–201.
32 S. Loeb, F. Van Hessen and D. Shahaf, *J. Membr. Sci.*, 1976, **1**, 249–269.
33 G. T. Gray, J. R. McCutcheon and M. Elimelech, *Desalination*, 2006, **197**, 1–8.
34 A. R. Hassan, N. a. Ali, N. Abdull and A. F. Ismail, *Desalination*, 2007, **206**, 107–126.
35 C. P. Koutsoua, S. G. Yiantsiosa and A. J. Karabelas, *J. Membr. Sci.*, 2009, **326**, 234–251.
36 J. R. McCutcheon and M. Elimelech, *J. Membr. Sci.*, 2006, **284**, 237–247.
37 C. H. Tan and H. Y. Ng, *J. Membr. Sci.*, 2008, **324**, 209–219.
38 C. D. Moody and J. O. Kessler, *Desalination*, 1976, **18**, 283–295.
39 J. O. Kessler and C. D. Moody, *Desalination*, 1976, **18**, 297–306.
40 J. O. Kessler and C. D. Moody, *Hydrol. Water Resour. Ariz. Southwest*, 1975, **5**, 91.
41 C. D. Moody, DPhil thesis, The University of Arizona, 1977.
42 G. W. Batchelder, *US Pat.*, 3171799, 1965.
43 D. N. Glew, *US Pat.*, 3216930, 1965.
44 B. S. Frank, *US Pat.*, 3670897, 1972.
45 W. T. Hough, *US Pat.*, 3721621, 1973.
46 R. E. Kravath and J. A. Davis, *Desalination*, 1975, **16**, 151–155.
47 http://www.businesswire.com/news/home/20100510005642/en/Oasys-Water-Commercializing-Osmosis-Membrane, 2010, vol. 2013.
48 http://www.reuters.com/article/2010/05/10/idUS132321+10-May-2010+BW20100510, Reuter, 2010, vol. 2013.
49 R. L. McGinnis, N. T. Hancock, M. S. Nowosielski-Slepowron and G. D. McGurgan, *Desalination*, 2013, **312**, 67–74.
50 I. Martin-Garcia, V. Monsalvo, M. Pidou, P. Le-Clech, S. J. Judd, E. J. McAdam and B. Jefferson, *J. Membr. Sci.*, 2011, **382**, 41–49.
51 O. A. Bamaga, A. Yokochi and E. G. Beaudry, *Desalin. Water Treat.*, 2009, **5**, 183–191.
52 O. A. Bamaga, A. Yokochi, B. Zabara and A. S. Babaqi, *Desalination*, 2011, **268**, 163–169.
53 E. Brauns, *Desalination*, 2008, **219**, 312–323.
54 T. Y. Cath, D. Adams and A. E. Childress, *J. Membr. Sci.*, 2005, **257**, 111–119.

55 T. Y. Cath, A. E. Childress and C. R. Martinetti, *US Pat.*, 20100224476A1, 2010.
56 E. R. Cornelissen, D. Harmsen, E. F. Beerendonk, J. J. Qin, H. Oo, K. F. de Korte and J. W. M. N. Kappelhof, *Water Sci. Technol.*, 2011, **63**, 1557–1565.
57 A. F. Emery and W. H. Yourstone Jr., Proceedings of the 18th Intersociety Energy Conversion Engineering Conference, 1983.
58 S. Gormly, J. Herron, M. Flynn, M. Hammoudeh and H. Shaw, *Desalin. Water Treat.*, 2011, **27**, 327–333.
59 R. W. Holloway, A. E. Childress, K. E. Dennett and T. Y. Cath, *Water Res.*, 2007, **41**, 4005–4014.
60 R. V. Linares, V. Yangali-Quintanilla, Z. Li and G. Amy, *Water Res.*, 2011, **45**, 6737–6744.
61 Z. Liu, H. Bai, J. Lee and D. D. Sun, *Energy Environ. Sci.*, 2011, **4**, 2582–2585.
62 J. R. McCutcheon, R. L. McGinnis and M. Elimelech, *Desalination*, 2005, **174**, 1–11.
63 C. A. Nayak and N. K. Rastogi, *Sep. Purif. Technol.*, 2010, **71**, 144–151.
64 L. Panyor, *Desalination*, 2006, **199**, 408–410.
65 M. Park, J. J. Lee, S. Lee and J. H. Kim, *J. Membr. Sci.*, 2011, **375**, 241–248.
66 K. Ravilious, *New Sci.*, 2010, **207**, 39–41.
67 Q. Schiermeier, *Nature*, 2008, **452**, 260–261.
68 S. E. Skilhagen, *Desalin. Water Treat.*, 2010, **15**, 271–278.
69 S. E. Skilhagen, J. E. Dugstad and R. J. Aaberg, *Desalination*, 2008, **220**, 476–482.
70 K. Y. Wang, M. M. Teoh, A. Nugroho and T.-S. Chung, *Chem. Eng. Sci.*, 2011, **66**, 2421–2430.
71 F. Zhang, K. S. Brastad and Z. He, *Environ. Sci. Technol.*, 2011, **45**, 6690–6696.
72 C. A. Nayak, S. S. Valluri and N. K. Rastogi, *J. Food Eng.*, 2011, **106**, 48–52.
73 A. Sagiv, N. Avraham, C. G. Dosoretz and R. Semiat, *J. Membr. Sci.*, 2008, **322**, 225–233.
74 A. Sagiv and R. Semiat, *Desalination*, 2005, **179**, 1–9.
75 A. Sagiv and R. Semiat, *Desalination*, 2010, **261**, 338–346.
76 Y. Liu and B. Mi, *J. Membr. Sci.*, 2012, **407–408**, 136–144.
77 B. Mi and M. Elimelech, *J. Membr. Sci.*, 2010, **348**, 337–345.
78 B. Mi and M. Elimelech, *Environ. Sci. Technol.*, 2010, **44**, 2022–2028.
79 S. Zou, Y. Gu, D. Xiao and C. Y. Tang, *J. Membr. Sci.*, 2011, **366**, 356–362.
80 T. Y. Cath and A. E. Childress, *US Pat.*, 7914680 B2, 2011.
81 T. Y. Cath and A. E. Childress, *US Pat.*, 8083942 B2, 2011.
82 T. Y. Cath, J. E. drewes and C. D. Lundin, *A novel hybrid forward osmosis process for drinking water augmentation using impaired water and saline water sources – final report*, Project # 4150, Water Research Foundation, Denver, CO., 2009.
83 D. L. Shaffer, N. Y. Yip, J. Gilron and M. Elimelech, *J. Membr. Sci.*, 2012, **415–416**, 1–8.
84 T.-w. Kim, Y. Kim, C. Yun, H. Jang, W. Kim and S. Park, *Desalination*, 2012, **284**, 253–260.
85 C. H. Tan and H. Y. Ng, *Desalin. Water Treat.*, 2010, **13**, 356–361.
86 P. McCormick, J. Pellegrino, F. Mantovani and G. Sarti, *J. Membr. Sci.*, 2008, **325**, 467–478.
87 R. L. McGinnis and M. Elimelech, *Desalination*, 2007, **207**, 370–382.
88 D. Li, X. Zhang, J. Yao, G. P. Simon and H. Wang, *Chem. Commun.*, 2011, **47**, 1710–1712.
89 D. Li, X. Zhang, J. Yao, Y. Zeng, G. P. Simon and H. Wang, *Soft Matter*, 2011, **7**, 10048–10056.
90 M. M. Ling and T.-S. Chung, *Desalination*, 2011, **278**, 194–202.
91 M. M. Ling and T.-S. Chung, *J. Membr. Sci.*, 2011, **372**, 201–209.
92 M. M. Ling, T.-S. Chung and X. Lu, *Chem. Commun.*, 2011, **47**, 10788–10790.
93 M. M. Ling, K. Y. Wang and T.-S. Chung, *Ind. Eng. Chem. Res.*, 2010, **49**, 5869–5876.
94 H. Bai, Z. Liu and D. D. Sun, *Sep. Purif. Technol.*, 2011, **81**, 392–399.
95 K. S. Bowden, A. Achilli and A. E. Childress, *Bioresour. Technol.*, 2012, **122**, 207–216.
96 S. Sarp, S. Lee, K. Park, M. Park, J. H. Kim and J. Cho, *Desalin. Water Treat.*, 2012, **43**, 131–137.
97 S. K. Yen, F. M. N. Haja, M. Su, K. Y. Wang and T.-S. Chung, *J. Membr. Sci.*, 2010, **364**, 242–252.
98 Q. Ge, J. Su, G. L. Amy and T.-S. Chung, *Water Res.*, 2012, **46**, 1318–1326.
99 S. Iyer, *US Pat.*, 2010015529, 2010.
100 R. L. McGinnis, J. R. McCutcheon and M. Elimelech, *J. Membr. Sci.*, 2007, **305**, 13–19.
101 S. Adham, J. Oppenheimer, L. Liu and M. Kumar, *WateReuse Foundation Research Report*, 2007.
102 H. Bai, Z. Liu and D. D. Sun, *Sep. Purif. Technol.*, 2011, **81**, 392–399.
103 S. Phuntsho, H. K. Shon, S. Hong, S. Lee and S. Vigneswaran, *J. Membr. Sci.*, 2011, **375**, 172–181.
104 Q. Ge, P. Wang, C. Wan and T.-S. Chung, *Environ. Sci. Technol.*, 2012, **46**, 6236–6243.
105 S. S. Sablani, M. F. A. Goosen, R. Al-Belushi and M. Wilf, *Desalination*, 2001, **141**, 269–289.
106 W. A. Phillip, J. S. Young and M. Elimelech, *Environ. Sci. Technol.*, 2010, **44**, 5170–5176.
107 K. L. Lee, R. W. Baker and H. K. Lonsdale, *J. Membr. Sci.*, 1981, **8**, 141–171.
108 C. Y. Tang, Q. She, W. C. L. Lay, R. Wang, R. Field and A. G. Fane, *Desalination*, 2011, **283**, 178–186.
109 N. T. Hancock, P. Xu, D. M. Heil, C. Bellona and T. Y. Cath, *Environ. Sci. Technol.*, 2011, **45**, 8483–8490.
110 C. Y. Tang, Q. She, W. C. L. Lay, R. Wang and A. G. Fane, *J. Membr. Sci.*, 2010, **354**, 123–133.
111 J. R. McCutcheon and M. Elimelech, *J. Membr. Sci.*, 2008, **318**, 458–466.
112 J. R. McCutcheon, R. L. McGinnis and M. Elimelech, *J. Membr. Sci.*, 2006, **278**, 114–123.
113 J. R. McCutcheon and M. Elimelech, *Abstr. Pap. Am. Chem. Soc.*, 2004, **228**, U633.

114 A. Achilli, T. Y. Cath and A. E. Childress, *J. Membr. Sci.*, 2009, **343**, 42–52.
115 B. Gu, D. Y. Kim, J. H. Kim and D. R. Yang, *J. Membr. Sci.*, 2011, **379**, 403–415.
116 G. Schock and A. Miquel, *Desalination*, 1987, **64**, 339–352.
117 V. Gekas and B. Hallström, *J. Membr. Sci.*, 1987, **30**, 153–170.
118 M. C. Y. Wong, K. Martinez, G. Z. Ramon and E. M. V. Hoek, *Desalination*, 2012, **287**, 340–349.
119 E. M. V. Hoek, A. S. Kim and M. Elimelech, *Environ. Eng. Sci.*, 2002, **19**, 357–372.
120 N. Y. Yip, A. Tiraferri, W. A. Phillip, J. D. Schiffman and M. Elimelech, *Environ. Sci. Technol.*, 2010, **44**, 3812–3818.
121 C. Boo, S. Lee, M. Elimelech, Z. Meng and S. Hong, *J. Membr. Sci.*, 2012, **390–391**, 277–284.
122 N. T. Hancock and T. Y. Cath, *Environ. Sci. Technol.*, 2009, **43**, 6769–6775.
123 N. T. Hancock, W. A. Phillip, M. Elimelech and T. Y. Cath, *Environ. Sci. Technol.*, 2011, **45**, 10642–10651.
124 X. Jin, C. Y. Tang, Y. Gu, Q. She and S. Qi, *Environ. Sci. Technol.*, 2011, **45**, 2323–2330.
125 Q. She, X. Jin, Q. Li and C. Y. Tang, *Water Res.*, 2012, **46**, 2478–2486.
126 Q. She, X. Jin and C. Y. Tang, *J. Membr. Sci.*, 2012, **401–402**, 262–273.
127 N. Y. Yip and M. Elimelech, *Environ. Sci. Technol.*, 2011, **45**, 10273–10282.
128 J. S. Yong, W. A. Phillip and M. Elimelech, *J. Membr. Sci.*, 2012, **392–393**, 9–17.
129 J. R. McCutcheon, R. L. McGinnis and M. Elimelech, *Desalination*, 2005, **174**, 1–11.
130 M. F. Gruber, C. J. Johnson, C. Y. Tang, M. H. Jensen, L. Yde and C. Helix-Nielsen, *J. Membr. Sci.*, 2011, **379**, 488–495.
131 L. Shi, S. R. Chou, R. Wang, W. X. Fang, C. Y. Tang and A. G. Fane, *J. Membr. Sci.*, 2011, **382**, 116–123.
132 S. Zhao and L. Zou, *J. Membr. Sci.*, 2011, **379**, 459–467.
133 Y. Xu, X. Peng, C. Y. Tang, Q. S. Fu and S. Nie, *J. Membr. Sci.*, 2010, **348**, 298–309.
134 J. Su and T.-S. Chung, *J. Membr. Sci.*, 2011, **376**, 214–224.
135 B. S. Chanukya, S. Patil and N. K. Rastogi, *Desalination*, 2013, **312**, 39–44.
136 T. Thorsen and T. Holt, *J. Membr. Sci.*, 2009, **335**, 103–110.
137 R. A. Al-Juboori and T. Yusaf, *Desalination*, 2012, **302**, 1–23.
138 C. Y. Tang, T. H. Chong and A. G. Fane, *Adv. Colloid Interface Sci.*, 2011, 164.
139 B. Mi and M. Elimelech, *J. Membr. Sci.*, 2008, **320**, 292–302.
140 V. Parida and H. Y. Ng, *Desalination*, 2013, **312**, 88–98.
141 Y. Wang, F. Wicaksana, C. Y. Tange and A. G. Fane, *Environ. Sci. Technol.*, 2010, **44**, 7102–7109.
142 Z.-Y. Li, V. Yangali-Quintanilla, R. Valladares-Linares, Q. Li, T. Zhan and G. Amy, *Water Res.*, 2012, **46**, 195–204.
143 J. T. Arena, B. McCloskey, B. D. Freeman and J. R. McCutcheon, *J. Membr. Sci.*, 2011, **375**, 55–62.
144 K. P. Lee, T. C. Arnot and D. Mattia, *J. Membr. Sci.*, 2011, **370**, 1–22.
145 D. Li and H. Wang, *J. Mater. Chem.*, 2010, **20**, 4551–4566.
146 M. Elimelech and R. McGinnis, *Membr. Technology*, 2009, **2009**, 10–11.
147 T. Thorsen and T. Holt, *J. Membr. Sci.*, 2009, **335**, 103–110.
148 J. Wei, C. Qiu, C. Y. Tang, R. Wang and A. G. Fane, *J. Membr. Sci.*, 2011, **372**, 292–302.
149 H. Lee, Y. Lee, A. R. Statz, J. Rho, T. G. Park and P. B. Messersmith, *Adv. Mater.*, 2008, **20**, 1619–1623.
150 B. D. McFloskey, H. B. Park, H. Ju, B. W. Rowe, D. J. Miller, B. J. Chun, K. Kin and B. D. Freeman, *Polymer*, 2010, **51**, 3472–3485.
151 D. Rana and T. Matsuura, *Chem. Rev.*, 2010, **110**, 2449–2471.
152 T. Y. Cath, M. Elimelech, J. R. McCutcheon, R. L. McGinnis, A. Achilli, D. Anastasio, A. R. Brady, A. E. Childress, I. V. Farr, N. T. Hancock, J. Lampi, L. D. Nghiem, M. Xie and N. Y. Yip, *Desalination*, 2012, **312**, 31–38.
153 S. Zhang, K. Y. Wang, T.-S. Chung, H. Chen, Y. C. Jean and G. Amy, *J. Membr. Sci.*, 2010, **360**, 522–535.
154 K. Y. Wang, R. C. Ong and T.-S. Chung, *Ind. Eng. Chem. Res.*, 2010, **49**, 4824–4831.
155 M. Sairam, E. Sereewatthanawut, K. Li, A. Bismarck and A. G. Livingston, *Desalination*, 2011, **273**, 299–307.
156 J. Herren, *US Pat.*, US7445712 B2, 2008.
157 C. Qiu, L. Setiawan, R. Wang, C. Y. Tang and A. G. Fane, *Desalination*, 2012, **287**, 266–270.
158 R. Wang, L. Shi, C. Y. Tang, S. Chou, C. Qiu and A. G. Fane, *J. Membr. Sci.*, 2010, **355**, 158–167.
159 A. Tiraferri, N. Y. Yip, W. A. Phillip, J. D. Schiffman and M. Elimelech, *J. Membr. Sci.*, 2011, **367**, 340–352.
160 N. Ma, J. Wei, R. Liao and C. Y. Tang, *J. Membr. Sci.*, 2012, **405–406**, 149–157.
161 K. Y. Wang, T.-S. Chung and G. Amy, *AIChE J.*, 2012, **58**, 770–781.
162 N. Widjojo, T.-S. Chung, M. Weber, C. Maletzko and V. Warzelhan, *J. Membr. Sci.*, 2011, **383**, 214–223.
163 X. Song, Z. Liu and D. D. Sun, *Adv. Mater.*, 2011, **23**, 3256–3260.
164 X. Li, K. Y. Wang, B. Helmer and T.-S. Chung, *Ind. Eng. Chem. Res.*, 2012, **51**, 10039–10050.
165 Q. Saren, C. Q. Qin and C. Y. Tang, *Environ. Sci. Technol.*, 2011, **45**, 5201–5208.
166 C. Qiu, S. Qi and C. Y. Tang, *J. Membr. Sci.*, 2011, **381**, 74–80.
167 S. Qi, C. Q. Qiu, Y. Zhao and C. Y. Tang, *J. Membr. Sci.*, 2012, **405–406**, 20–29.
168 S. Chou, L. Shi, R. Wang, C. Y. Tang, C. Qiu and A. G. Fane, *Desalination*, 2010, **261**, 365–372.
169 S. Chou, R. Wang, L. Shi, Q. She, C. Tang and A. G. Fane, *J. Membr. Sci.*, 2012, **389**, 25–33.
170 P. Sukitpaneenit and T.-S. Chung, *Environ. Eng. Sci.*, 2012, **46**, 7358–7365.
171 W. Fang, R. Wang, S. Chou, L. Setiawan and A. G. Fane, *J. Membr. Sci.*, 2012, **394–395**, 140–150.

172 I. F. J. Vankelecom, K. De Smet, L. E. M. Gevers and P. A. Jacobs, in *Nanofiltration principles and applications*, ed. A. I. Schafer, A. G. Fane and T. D. Waite, CPI Antony Rowe, Eastbourne, 2005, pp. 32–65.
173 A. Cano-Odena, M. Spilliers, T. Dedroog, K. De Grave, J. Ramon and I. F. J. Vankelecom, *J. Membr. Sci.*, 2011, **366**, 25–32.
174 S. Zhang, K. Y. Wang, T.-S. Chung, Y. C. Jean and H. Chen, *Chem. Eng. Sci.*, 2011, **66**, 2008–2018.
175 E. Saljoughi, M. Sadrzadeh and T. Mohammadi, *J. Membr. Sci.*, 2009, **326**, 627–634.
176 T. Mohammadi and E. Saljoughi, *Desalination*, 2009, **243**, 1–7.
177 G. Arthanareeswaran and S. Ananda Kumar, *J. Porous Mater.*, 2010, **17**, 515–522.
178 A. Rahimpour and S. S. Madaeni, *J. Membr. Sci.*, 2007, **305**, 299–312.
179 R. C. Ong and T.-S. Chung, *J. Membr. Sci.*, 2012, **394–395**, 230–240.
180 W. Li, Y. Gao and C. Y. Tang, *J. Membr. Sci.*, 2011, **379**, 307–321.
181 P. Aerts, I. Genné, R. Leysen, P. A. Jacobs and I. F. J. Vankelecom, *J. Membr. Sci.*, 2006, **283**, 320–327.
182 C. J. Kurth and R. L. Burk, *US Pat.*, 2009/0272692 A1, 2009.
183 Y. Yu, S. Seo, I.-C. Kim and S. Lee, *J. Membr. Sci.*, 2011, **375**, 63–68.
184 X. Wei, Z. Wang, J. Chen, J. Wang and S. Wang, *J. Membr. Sci.*, 2010, **346**, 152–162.
185 A. K. Ghosh and E. M. V. Hoek, *J. Membr. Sci.*, 2009, **336**, 140–148.
186 N.-N. Bui, M. L. Lind, E. M. V. Hoek and J. R. McCutcheon, *J. Membr. Sci.*, 2011, **385–386**, 10–19.
187 L. A. Hoover, J. D. Schiffman and M. Elimelech, *Desalination*, 2013, **308**, 73–81.
188 L. Chen, L. Bromberg, T. A. Hatton and G. C. Rutledge, *Polymer*, 2008, **49**, 1266–1275.
189 I. S. Chronakis, *J. Mater. Process. Technol.*, 2005, **167**, 283–293.
190 V. A. Ganesh, H. K. Raut, A. S. Nair and S. Ramakrishna, *J. Mater. Chem.*, 2011, **21**, 16304–16322.
191 K. C. Krogman, J. L. Lowery, N. S. Zacharia, G. C. Rutledge and P. T. Hammond, *Nat. Mater.*, 2009, **8**, 512–518.
192 J. A. Lee, K. C. Krogman, M. Ma, R. M. Hill, P. T. Hammond and G. C. Rutledg, *Adv. Mater.*, 2009, **21**, 1252–1256.
193 W. J. Lau, A. F. Ismail, N. Misdan and M. A. Kassim, *Desalination*, 2012, **287**, 190–199.
194 J. Wei, X. Liu, C. Qiu, R. Wang and C. Y. Tang, *J. Membr. Sci.*, 2011, **381**, 110–117.
195 C. Kong, M. Kanezashi, T. Yamomoto, T. Shintani and T. Tsuru, *J. Membr. Sci.*, 2010, **362**, 76–80.
196 A. P. Rao, N. V. Desai and R. Rangarajan, *J. Membr. Sci.*, 1997, **124**, 263–272.
197 J. Jegal, S. G. Min and K.-H. Lee, *J. Appl. Polym. Sci.*, 2002, **86**, 2781–2787.
198 H. I. Kim and S. S. Kim, *J. Membr. Sci.*, 2006, **286**, 193–201.
199 A. K. Ghosh, B.-H. Jeong, X. Huang and E. M. V. Hoek, *J. Membr. Sci.*, 2008, **311**, 34–45.
200 L. Meihong, Y. Sanchuan, Z. Yong and G. Congjie, *J. Membr. Sci.*, 2008, **310**, 289–295.
201 E.-S. Kim and B. Deng, *J. Membr. Sci.*, 2011, **375**, 46–54.
202 N.-W. OH, J. Jegal and K.-H. Lee, *J. Appl. Polym. Sci.*, 2001, **80**, 2729–2736.
203 H.-J. Oh, J. Jegal and K.-H. Lee, *J. Appl. Polym. Sci.*, 2001, **80**, 1854–1862.
204 B.-H. Jeong, E. M. V. Hoek, Y. Yan, A. Subramani, X. Huang, G. Hurwitz, A. K. Ghosh and A. Jawor, *J. Membr. Sci.*, 2007, **294**, 1–7.
205 H. S. Lee, S. J. Im, J. H. Kim, H. J. Kim, J. P. Kim and B. R. Min, *Desalination*, 2008, **219**, 48–56.
206 G. L. Jadav and P. S. Singh, *J. Membr. Sci.*, 2009, **328**, 257–267.
207 R. Revanur, I. Roh, J. E. Klare, A. Noy and O. Bakajin, *US Pat.*, 20120080378A1, 2012.
208 W. C. L. Lay, Q. Zhang, J. Zhang, D. McDougald, C. Tang, R. Wang, Y. Liu and A. G. Fane, *Desalination*, 2011, **283**, 123–130.
209 L. S. Penn and H. Wang, *Polym. Adv. Technol.*, 1994, **5**, 809–817.
210 L. Setiawan, R. Wang, K. Li and A. G. Fane, *J. Membr. Sci.*, 2011, **369**, 196–205.
211 L. Setiawan, R. Wang, K. Li and A. G. Fane, *J. Membr. Sci.*, 2012, **394–395**, 80–88.
212 M. L. Bruening, D. M. Dotzauer, P. Jain, L. Ouyang and G. L. Baker, *Langmuir*, 2008, **24**, 7663–7673.
213 P. Ott, J. Gensel, S. Roesler, K. Trenkenschuh, D. Andreeva, A. Laschewsky and A. Fery, *Chem. Mater.*, 2010, **22**, 3323–3331.
214 P. Vandezande, L. E. M. Gevers and I. F. J. Vankelecom, *Chem. Soc. Rev.*, 2007, **37**, 365–405.
215 P. Vandezande, X. Li, L. E. M. Gevers and I. F. J. Vankelecom, *J. Membr. Sci.*, 2009, **330**, 307–318.
216 M. Liu, S. Yu, J. Tao and C. Gao, *J. Membr. Sci.*, 2008, **325**, 947–956.
217 S. Yu, M. Liu, X. Liu and C. Gao, *J. Membr. Sci.*, 2009, **342**, 313–320.
218 G. M. Geise, H. B. Park, A. C. Sagle, B. D. Freeman and J. E. McGrath, *J. Membr. Sci.*, 2011, **369**, 130–138.
219 W. Xie, J. Cook, H. B. Park, B. D. Freeman, C. H. Lee and J. E. McGrath, *Polymer*, 2011, **52**, 2032–2043.
220 J. E. Miller and L. R. Evan, *Forward osmosis: a new approach to water purification and desalination*, Sandia National Laboratories, Virginia, 2006.
221 http://www.nasa.gov/mission_pages/station/research/experiments/FOB.html.
222 Statkraft, The 3rd osmosis membrane summit, Barcelona, 2012.
223 http://www.htiwater.com/company/hti_history.html.